ACS NANO
Cite This: ACS Nano 2018, 12, 2728–2740
www.acsnano.org

ARTICLE

Multiwall Carbon Nanotubes Induce More Pronounced Transcriptomic Responses in *Pseudomonas aeruginosa* PG201 than Graphene, Exfoliated Boron Nitride, or Carbon Black

Monika Mortimer,[†,‡] Naresh Devarajan,[†] Dong Li,[†] and Patricia A. Holden*[,†,‡]

[†]Bren School of Environmental Science and Management and Earth Research Institute and [‡]University of California Center for the Environmental Implications of Nanotechnology (UC CEIN), University of California, Santa Barbara, California 93106, United States

Supporting Information

ABSTRACT: Carbonaceous and boron nitride (BN) nanomaterials have similar applications and hydrophobic properties suggesting common release pathways and exposure to bacteria. While high nanomaterial concentrations can be bactericidal or growth-inhibitory, little is known regarding bacterial transcriptional responses to non-growth-inhibitory nanomaterial concentrations. Here, using one strain of *Pseudomonas aeruginosa*—a clinically and environmentally important bacterial taxon—we analyzed the comparative transcriptomic response to carbonaceous or BN nanomaterials. We show that, at non-growth-inhibitory, equal mass concentrations (10 mg/L), multiwall carbon nanotubes (MWCNTs) induced differential regulation of 111 genes in *P. aeruginosa*, while graphene, BN, and carbon black caused differential regulation of 44, 26, and 25 genes, respectively. MWCNTs caused the upregulation of genes encoding general stress response (9 genes), sulfur metabolism (15), and transport of small molecules (7) and downregulation of genes encoding flagellar basal-body rod proteins and other virulence-related factors (6), nitrogen metabolism (7), and membrane proteins (12), including a two-component regulatory system CzcS/R. Because two-component systems are associated with antibiotic resistance, the antibiotic susceptibility of *P. aeruginosa* was tested following MWCNT exposure. In MWCNT-treated cultures, the minimal inhibitory concentrations (MICs) of meropenem and imipenem decreased from 0.06 to 0.03 μg/mL and from 0.25 to 0.125 μg/mL, respectively. Taken together, whole genome analysis indicated that, in the absence of growth inhibition, nanomaterials can alter bacterial physiology and metabolism. For MWCNTs, such alterations may include downregulation of antibiotic resistance pathways, suggesting that pre-exposure to MWCNTs could potentially render bacteria more susceptible to carbapenems which are often the last resort for the globally concerning, highly antibiotic resistant *P. aeruginosa*.

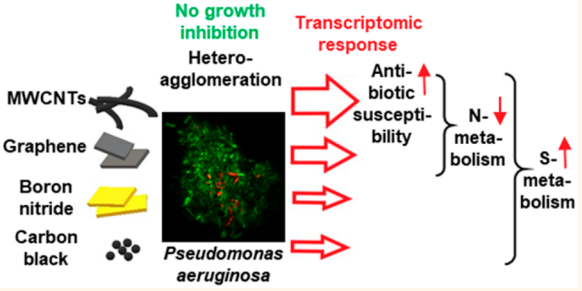

KEYWORDS: *carbon nanotubes, graphene, boron nitride, carbon black, bacteria, transcriptomics*

As carbon-based nanomaterials (NMs), including engineered multiwall carbon nanotubes (MWCNTs) and graphene plus industrial amorphous carbon black (CB), are increasingly used, such NMs are undoubtedly entering the environment. Based on models and measurements, carbonaceous NM environmental concentrations are expected to range from less than 0.001 mg/L in water to approximately 1 mg/kg in solid media such as soils and biosolids.[1,2] Hexagonal boron nitride (BN) nanosheets are structural and isoelectric analogues of graphene with similar uses such as multifunctional coatings and polymer additives.[3] Although carbonaceous and BN NMs chemically differ, their similar applications and key characteristics of insolubility plus morphotypes including nanotubes and flakes suggest in-common release pathways, including to soils via atmospheric deposition and fertilization by wastewater treatment plant (WWTP) biosolids.[4] Thus, environmental exposures to biota will occur, particularly to bacteria which are environmentally ubiquitous including in soils.[5,6] Generally, NMs could alter bacterial physiology and associated nutrient cycling metabolisms, induce microbial community shifts,[5] and

Received: December 19, 2017
Accepted: February 18, 2018
Published: February 19, 2018

DOI: 10.1021/acsnano.7b08977
ACS Nano 2018, 12, 2728–2740

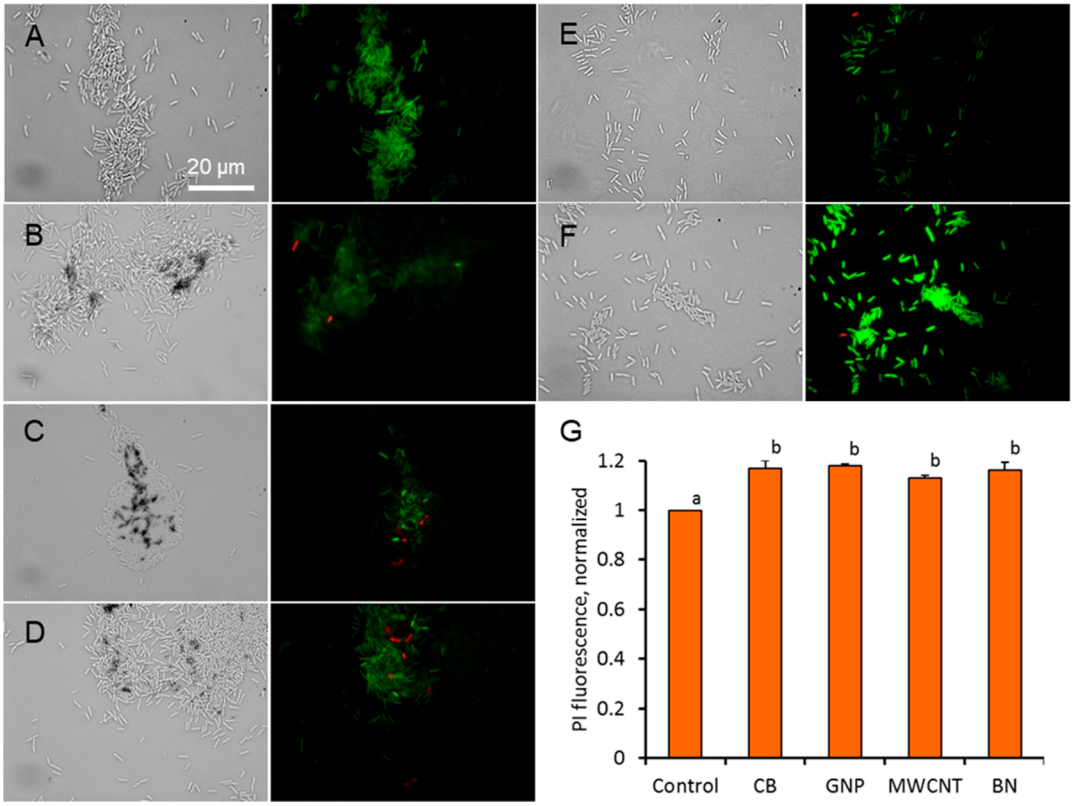

Figure 1. (A–F) Bright field (grayscale) and fluorescence (red and green) images of *P. aeruginosa* after SYTO9 (green) and propidium iodide (PI, red) staining and (G) relative amount of PI-stained (membrane-damaged) bacteria in the cultures grown without (control) and with nanomaterials (NMs). *P. aeruginosa* was grown as (A) an unamended control culture or with 10 mg/L (B) MWCNTs, (C) carbon black (CB), (D) graphene nanoplatelets (GNP), (E) boron nitride flakes (BN), or (F) 20 mg/L alginic acid for 5 h, and wet mounts were prepared of PI/SYTO9 stained cells. Dark agglomerates in B–D are carbon-based NMs. Because SYTO9 fluorescence was quenched in NM-containing cultures, SYTO9/PI ratios may have overestimated the membrane damage caused by NMs. (G) Assuming equal cell concentrations in all of the treatments and control, based on the growth assays, PI fluorescence instead of the ratio of SYTO9/PI fluorescence is presented; different letters indicate significantly different values ($p < 0.05$).

affect plant-microbe interactions;[7] bacteria could also physically affect NM partitioning in environmental compartments and could promote NM exposure to higher organisms by initiating trophic transfer.[6,8] For these reasons, mechanisms of bacterial interactions with carbonaceous and BN NMs should be understood.

The toxicity of various carbonaceous NMs to bacteria has been reported,[9−15] indicating that antibacterial properties of carbonaceous NMs are related to NM physicochemical characteristics. While comparatively little is known regarding BN NMs, MWCNTs are generally reported as less toxic than single wall carbon nanotubes (SWCNTs), and functionalized carbon nanotubes and graphene are more damaging to bacteria than their unfunctionalized or reduced counterparts.[16] However, there are inconsistencies within NM types, *i.e.*, in *Escherichia coli* where either aggregated metallic SWCNTs at 1 mg/L caused membrane-associated oxidative stress[17] or dispersed, metallic or semiconductor, SWCNTs at 100 mg/L neither impeded growth nor damaged membranes.[18] Similarly, CB, an industrial carbonaceous NM widely applied as a pigment and used to reinforce tires and thus relatively environmentally abundant, was deemed non-bioaccumulative and nontoxic to aquatic organisms because the predicted environmental concentrations were found to be lower than no-effect concentrations that were greater than 1000 mg/L in aquatic toxicity tests.[19] However, CB-amended soils have been reported to affect soil bacterial communities at 1000 mg/kg of CB and result in impaired soybean N_2 fixation potentials at 0.1 and 100 mg/kg of CB, suggesting that CB has soil biotic effects that are comparable to MWCNTs and graphene.[5,7]

Investigating mechanisms of NM bioeffects is afforded by gene transcriptional analyses.[20] Even in cases of modest antibacterial effects, NMs can induce significant changes in gene expression regulation in bacteria.[21,22] Growth inhibition and decreased denitrification activity in *Paracoccus denitrificans*, caused by the exposure to 50 mg/L of carboxylated SWCNTs, were shown to correlate with the upregulation of genes involved in DNA repair and the downregulation of glucose metabolism and nitrate reductase genes.[23] Both SWCNTs and MWCNTs at concentrations of 20 mg/L were shown to induce high levels of stress-related gene transcriptional activity in *E. coli*.[21] The two latter reports and other studies of NM-exposed bacteria have used transcriptional analysis for interpreting observed physiological responses to NMs, *i.e.*, by conducting whole genome analyses of bacteria after exposures to growth-inhibitory concentrations of NMs. Further, most of the gene expression studies in NM-exposed microorganisms have focused on intrinsically antibacterial metal NMs.[20] For instance, exposure to nanosized silver has been reported to upregulate antioxidant synthesis and heat shock responses, copper homeostasis, sulfate transport and assimilation, and antibiotic resistance pathways in *E. coli*.[24,25] In addition, CdSe-ZnS

DOI: 10.1021/acsnano.7b08977
ACS Nano 2018, 12, 2728–2740

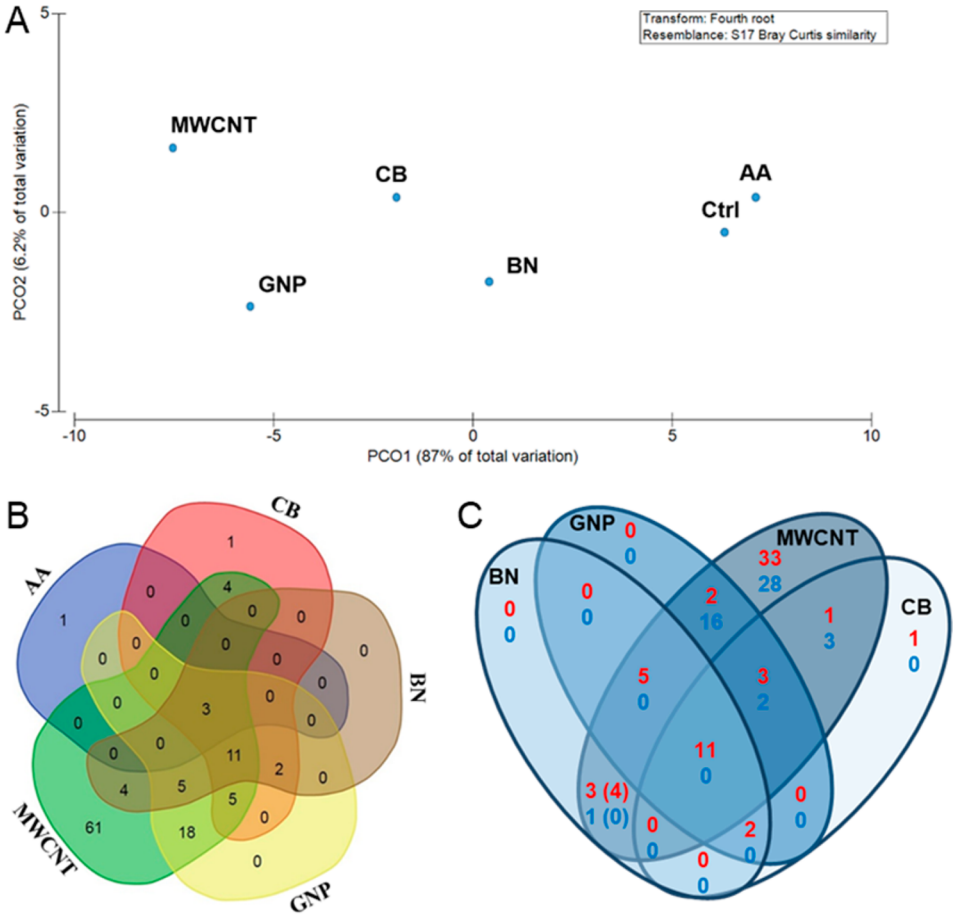

Figure 2. Gene expression in *P. aeruginosa* PG201 exposed to four nanomaterials (NMs) and alginic acid (AA, alginic acid; CB, carbon black; BN, boron nitride; GNP, graphene nanoplatelets; MWCNT, multiwall carbon nanotubes; and Ctrl, unamended culture). (A) Principal coordinates analysis based on the number of genes with a $\log_2$(fold change) ≥ 1.4 or ≤−1.4 and a multiple testing adjusted *p*-value below 0.05. Venn diagrams showing (B) the number of differentially regulated genes in *P. aeruginosa* PG201 in response to the four NMs and AA compared to the unamended culture and (C) number of upregulated (red) and downregulated (blue) genes in response to each NM compared to the unamended culture. In all cases but one, the up- and downregulation patterns were the same across the NMs, although one hypothetical protein was downregulated by BN but upregulated by MWCNTs as indicated by the numbers in parentheses.

quantum dots induced antibiotic resistance gene transcription in *Pseudomonas aeruginosa* PAO1.[22] The upregulation of antibiotic resistance-related genes by metal NMs highlights the need for better understanding NM antibacterial mechanisms to avoid unwanted consequences such as contributing to antibacterial resistance in the environment by application of metal NM-enabled agricultural products. Thus, further transcriptomics-based studies are needed, especially regarding sublethal effects of nonmetal NMs on bacteria, since only a few reports are available.

Here, we applied RNA sequencing (RNA-seq) to *P. aeruginosa* PG201 cultured with MWCNTs, graphene nanoplatelets (GNPs), CB, or hexagonal BN flakes at sublethal, nongrowth-inhibitory concentrations to shed light on the potential resistance mechanisms and cellular responses to NM exposure not evident at the physiological level. Further, based on the transcriptomics results, the effects on carbapenem susceptibility of *P. aeruginosa* PG201 were studied. *P. aeruginosa* as a versatile bacterial species capable of colonizing diverse environments[26] and as an opportunistic pathogen[27] serves as an excellent model for NM environmental effect and health studies. Our results indicate that, when exposed to NMs at a sublethal concentration, the gene transcriptional responses of *P. aeruginosa* to MWCNTs, GNPs, CB, and BN flakes were NM-specific yet comparatively pronounced with MWCNTs.

RESULTS AND DISCUSSION

Characteristics of NMs. MWCNTs, GNPs, BN, and CB were stably dispersed in nanopure water with alginic acid (AA). CB, BN, and GNPs remained well dispersed after dilution into the bacterial growth medium with hydrodynamic diameters similar to those measured in nanopure water (Table S1). MWCNTs, differently from other NMs, agglomerated to the micrometer size range in the growth medium. However, the hydrodynamic diameters of NMs in the growth medium did not reflect the agglomeration pattern of NMs in the bacterial cultures as discussed below. The physicochemical properties and proven biocompatibility of AA-dispersed NMs are provided elsewhere.[28]

NMs Did Not Inhibit Bacterial Growth. When NM dispersions were inoculated with *P. aeruginosa* PG201 in mineral growth medium, the NMs rapidly agglomerated with bacteria, consistent with the literature.[29] Even though the formation of NM−bacteria heteroagglomerates caused heterogeneous exposure in the bacterial cultures, it occurred for all of the tested NMs (Figure 1), irrespective of the NM hydro-

DOI: 10.1021/acsnano.7b08977
ACS Nano 2018, 12, 2728−2740

dynamic diameters measured in abiotic growth media (Table S1). Consequently, the NM exposures were comparable and indicative of environmentally relevant conditions where NM−bacteria heteroagglomeration is expected.[29] Due to the agglomeration of bacterial cells, assessing growth by standard methods, such as optical density measurements or direct cell counts, was not feasible. Instead, ATP concentrations were measured in the cultures over time to construct growth curves (Figure S1). The suitability of ATP as a proxy for bacterial growth was first validated using unamended control and cadmium-exposed cultures, showing that ATP concentrations and optical densities at 600 nm (OD_{600}) measured over the exponential growth phase (up to 10 h) were significantly positively correlated (Figure S2). Further, the specific growth rates calculated based on ATP concentrations for control and cadmium-exposed cultures (Table S2) were not significantly different from the values calculated based on OD_{600} measurements (Table S2).

Based on the specific growth rates calculated from time course ATP concentrations (Figure S1 and Table S2), the NMs were not growth-inhibitory to *P. aeruginosa* at NM concentrations up to 10 mg/L. This is consistent with literature reports where MWCNTs have been found to minimally impact bacteria compared to SWCNTs.[11] Concentrations of MWCNTs up to 500−875 mg/L did not affect the viability of *Salmonella typhimurium* or *Bacillus subtilis* during a 1-h exposure[11] or the viability of stress-resistant *Cupriavidus metallidurans* during a 24-h exposure.[30] The threshold MWCNT antibacterial concentration in *E. coli* was reportedly as high as 100 mg/L.[30] For demonstrating antibacterial activity of graphene in suspensions, concentrations in the range of 100−5000 mg/L have been used.[31,32] BN has been reported as relatively benign in eukaryotic cell systems and *in vivo* studies.[33] The only study that has reported antibacterial activity of BN nanotubes used polyethylenimine (PEI)-coated BN nanotubes at very high concentrations of 100−1000 mg/L, and PEI was found to be the cause of toxicity.[34]

NMs Moderately Damaged Bacterial Membranes. Even though the specific growth rate of *P. aeruginosa* PG201 was not affected in the presence of NMs, NM−bacterial heteroagglomerate formation was evident. Based on published reports, the antibacterial activity of carbon-based NMs is mainly mediated by direct contact between NMs and bacteria, and the toxicity is determined by physicochemical properties of NMs.[9,10,31,35] Graphene oxide and MWCNTs have been shown to damage bacterial membranes.[9,32] Here, the mode of AA adsorption to the surfaces of NMs was expected to leave pristine NM surfaces partly exposed for interactions with bacteria,[28] likely via hydrophobic interactions. This prompted assessing the potential membrane damage of *P. aeruginosa* in NM-exposed cultures by propidium iodide (PI) staining of bacteria grown with 10 mg/L of NMs for 5 h. A statistically significant ($p < 0.05$) 13−18% increase in PI fluorescence compared to unamended control cultures was detected upon NM exposure as quantified fluorometrically and illustrated by microscopic imaging (Figure 1). However, PI-permeable membranes do not necessarily indicate dead or irreparably damaged cells.[36] Considering that NMs were not growth-inhibitory to *P. aeruginosa* and that there was no statistically significant difference between PI fluorescence induced by each NM (Figure 1G), the increase in PI stained cells in NM-exposed cultures compared to control indicated a nonspecific physical interaction between NMs and bacteria. To further evaluate the potential specificity of *P. aeruginosa* responses to the high nongrowth-inhibitory NM concentration (10 mg/L) and to shed light on the potential resistance mechanisms or cellular responses that were not evident at the physiological level, we conducted a transcriptomic analysis of NM-exposed bacteria.

Alginic Acid (AA) Did Not Contribute Substantially to the Transcriptomic Response of *P. aeruginosa* Exposed to AA-Coated NMs. AA was included as a separate treatment to differentiate gene expression changes induced by AA coating on the NMs *versus* the changes caused by NMs. Principal coordinates (PCO) analysis confirmed the similarities in the gene expression profiles of unamended control culture and AA treatment (Figure 2A). PCO analysis also indicated that the gene expression patterns in NM-exposed cultures were clearly distinct from those of the control and AA-exposed cultures, with MWCNT-exposed culture most distinct from the control. AA induced upregulation of only four genes, including three that were commonly also induced by NMs (Figure 2B), indicating that the contribution of AA to gene expression in NM treatments was minimal. The AA treatment coincided with three upregulated genes: PA3450 encoding a probable antioxidant protein 1-cysteine peroxiredoxin LsfA, PA3446 encoding a conserved hypothetical protein resembling SsuE with a flavin mononucleotide reductase activity, and PA0284, a hypothetical protein with unknown function (Table S3). The upregulation of these genes in the NM treatments was higher than in the AA treatment with $\log_2$(fold change) values approximately two times higher in the NM treatments. Only one gene was distinctively upregulated by AA: *exaA* (PA1982), which belongs to a carbon compound catabolism functional group and has been associated with ethanol oxidation.[37]

***P. aeruginosa* Global Transcriptomic Response to NMs.** The total numbers of differentially regulated genes were as follows: 111 (62 up- and 49 down-regulated) in the MWCNT treatment; 44 (26 up- and 18 downregulated) in the GNP treatment; 26 (21 up- and 5 downregulated) in the CB treatment; and 25 (all upregulated) in the BN treatment. In general, the number of up- and down-regulated genes was consistent with literature reports regarding whole-genome studies of bacteria exposed to NMs at low toxicity concentrations. Pelletier *et al.*[38] reported 2-fold or greater differences in the expression of 62 genes in *E. coli* after 1-h exposure to 100 mg/L of CeO_2 NPs that induced a slight inhibition of cell growth. RNA-seq of *P. denitrificans* indicated significant up- or down-regulation of 37 genes after growth with 50 mg/L of carboxylated SWCNTs.[23] Other short-term stressors, for instance, 30 min heat shock at 46 °C, have induced differential expression of 133 genes in *P. aeruginosa*.[39] Some studies have reported up- and downregulation of higher numbers of genes: 966 genes were affected in *Legionella pneumophila* in response to CuO NP exposure (160 mg/L for 3 h)[40] and 438 genes in *E. coli* in response to 20 mg/L MWCNTs for 4 h.[21] Metal-based NPs, especially Ag- and Cu-based that are known to exert antibacterial effects, expectedly induce more pronounced transcriptomic response in bacteria. On the other hand, much lower numbers of genes were affected in response to MWCNTs in this study compared to the work of Kang *et al.*;[21] in addition to the intrinsic properties of specific MWCNTs, this might be explained by differences in the ratio of bacteria to MWCNTs and the exposure medium, *i.e.*, growth medium *versus* the diluted medium not supporting growth used by Kang *et al.* Here, MWCNTs distinctively regulated 61 genes

DOI: 10.1021/acsnano.7b08977
ACS Nano 2018, 12, 2728−2740

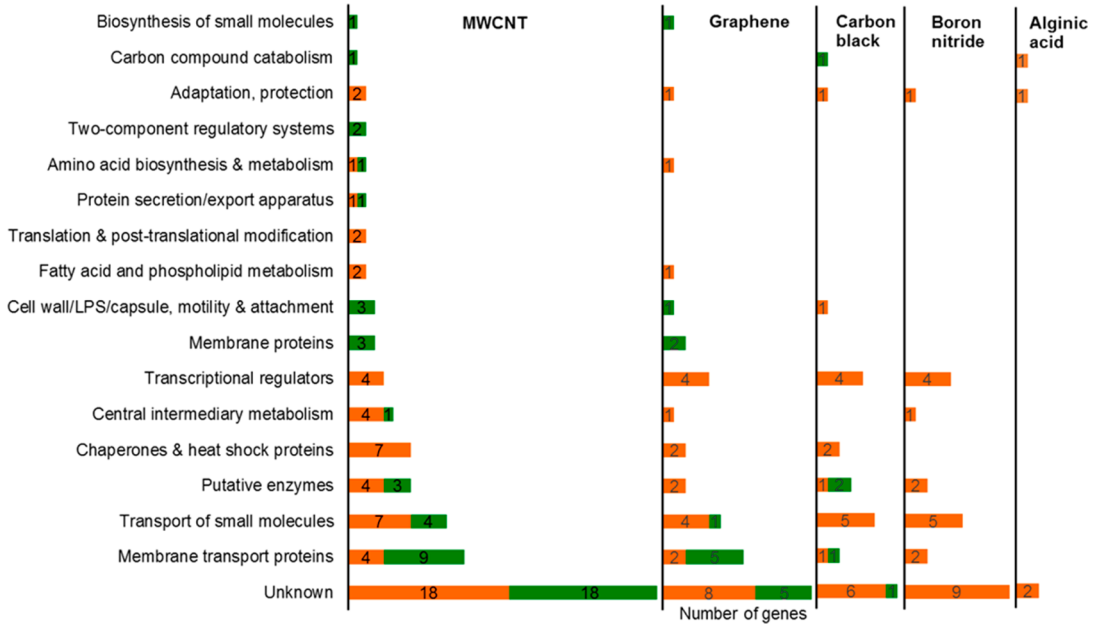

Figure 3. Distribution of nanomaterial- and alginic acid-exposed *P. aeruginosa* upregulated (orange) and downregulated (green) transcripts by functional classes (data from Table S3). Functional classes were assigned on the basis of the *Pseudomonas* Genome Database. LPS, lipopolysaccharides.

(33 up- and 28 downregulated), which differed from the other NMs that only distinctively regulated one gene (CB) or did not induce any unique responses in gene expression (GNPs and BN, Figure 2B and C).

All NMs Regulated Genes of Membrane Transport Proteins, Other Transporters of Small Molecules and Transcriptional Regulators. The most pronounced set of commonly regulated genes was induced by GNPs and MWCNTs (2 up- and 16 downregulated, Figure 2C), suggesting similarities in their mode of action. Comparison of the gene sets coinduced by MWCNTs and other NMs or by pairs of other NMs showed that commonly regulated gene sets either did not exist or were very small, *i.e.*, under five genes. All four NMs induced upregulation of 11 common genes that can be interpreted as a general response to NMs. These genes belonged to functional groups of transcriptional regulators (four genes) and transport of small molecules (four genes), one putative enzyme, and two genes of unknown function (Figure 3 and Table S3).

Three carbonaceous NMs, MWCNTs, GNPs, and CB, commonly upregulated three and downregulated two transcripts (Figure 2C). Among these were genes encoding transcripts of probable metal-transporting P-type ATPase (PA3690) and aquaporin Z *aqpZ* (PA4034) belonging to the group of membrane transport proteins (Figure 3 and Table S3). In addition, the genes of ATP-dependent protease subunit HslV (PA5053) and heat shock protein GrpE (PA4762), both in the functional category of chaperones and heat shock proteins, were upregulated by the carbonaceous NMs. HslV is a protease subunit of a proteasome-like degradation complex, believed to be a general protein degrading apparatus, and GrpE participates actively in the response to hyperosmotic and heat shock by preventing the aggregation of stress-denatured proteins. AqpZ is a channel that permits osmotically driven movement of water in both directions and is involved in osmoregulation and maintenance of cell turgor during volume expansion in rapidly growing cells.[41] Thus, the apparent carbonaceous NM-specific responses included osmoregulation and general stress response.

Carbonaceous and BN-Based NMs Upregulated Transcripts Involved in Sulfur Metabolism. 1D and 2D NMs, *i.e.*, MWCNTs, GNPs, and BN, commonly upregulated a set of five genes that was different from the set induced by all three carbonaceous NMs (Figure 2C). The genes belonged to the functional groups of membrane transport proteins (sulfate transport protein CysT, PA0282), central intermediary metabolism (sulfate adenylyltransferase subunit 2, CysD, PA4443), putative enzymes (alkanesulfonate monooxygenase, SsuD, PA3444), and genes of unknown function (conserved hypothetical proteins PA3445 and PA3449) (Figure 3 and Table S3). Interestingly, all of these genes, including the hypothetical proteins, were associated with sulfur metabolism. In general, all NM exposures appeared to upregulate several sulfur metabolism-associated genes (Table 1). Among these were genes responsible for transmembrane transport of extracellular sulfate (*cysT*, *cysP*, and *sbp*), taurine (*tauABC*), and alkanesulfonate (*ssuBCDEF*, PA3445, and PA 3449). The *ssuFBCDAE* locus is known to play a key role in organosulfur uptake in *Pseudomonas*.[42] Here, sulfate was provided as a sulfur source; hence, it was surprising that genes associated with the transport of taurine and organosulfur were upregulated in NM exposures. In addition to sulfur compound transport genes, genes involved in assimilatory sulfate reduction (*cysND*, *cysC*, and *cysH*) were upregulated (Figure S3). Genes involved in sulfur metabolism have been shown to be upregulated in response to sulfate starvation.[43,44] Similarly, upregulation of low-sulfur-content proteins (including *tauABCD*, *ssuABCDE*, and *cysP*) was detected upon sulfur starvation in *P. putida*.[45] Tralau *et al.*[44] found that sulfur starvation induced upregulation of a large family of genes, including genes encoding sulfatases, sulfonatases, transport systems, and oxidative stress proteins. Here, bacteria were not expected to suffer from sulfur starvation due to the relatively short culturing time. However, the possible adsorption of sulfates and other cations and anions by NMs in

DOI: 10.1021/acsnano.7b08977
ACS Nano 2018, 12, 2728−2740

Table 1. Differentially Regulated Genes [$\log_2$(fold change) ≥ 1.4 or ≤−1.4, $p < 0.05$] upon *P. aeruginosa* PG201 Growth with Nanomaterials for 5 h, Grouped by KEGG Metabolic Pathways[a]

KEGG module	$\log_2$(fold change in gene expression) MWCNT	GNP	BN	CB	gene	product
Energy Metabolism						
nitrogen metabolism	−1.6				PA1781	assimilatory nitrite reductase large subunit NirB
	−2.2	−2.3			PA1783	nitrate transporter NasA
	−1.9	−2.0			PA1785	antiterminator NasT
	−1.7	−1.8			PA1786	nitrate sensor NasS
	1.5				PA4864	urease accessory protein UreD
	−1.5	−1.6			PA4893	urease accessory protein UreG
	−1.6	−2.1			PA4894	hypothetical protein UreJ[b]
	−2.2	−2.0			PA5287	ammonium transporter AmtB
sulfur metabolism	3.4	1.9	2.9		PA0282	sulfate transport protein CysT
	4.1	3.5	4.0	2.3	PA0283	sulfate-binding protein precursor Sbp
	1.7				PA1493	sulfate-binding protein of ABC transporter CysP
	1.9	1.7			PA1756	3′-phosphoadenosine-5′-phosphosulfate reductase, CysH
	2.7	2.1	2.8	1.4	PA2062	probable pyridoxal-phosphate dependent enzyme
	1.6			1.5	PA3441	probable molybdopterin-binding protein SsuF
	1.8				PA3442,PA3443	probable ATP-binding component or permease of ABC transporter, YcbE, SsuB, YcbM, SsuC
	2.7	1.5	1.7		PA3444	alkanesulfonate monooxygenase SsuD
	3.5	2.4	3.0		PA3445	conserved hypothetical protein, transporter activity
	3.6	4.2	4.4	3.5	PA3446	conserved hypothetical protein SsuE
	3.0	2.0	2.6		PA3449	conserved hypothetical protein, transporter activity
	2.3		1.5		PA3936,PA3937	probable ATP-binding component or permease of ABC taurine transporter TauC, TauB
	3.6	3.3	3.4	2.6	PA3938	probable periplasmic taurine-binding protein precursor TauA
	1.8				PA4442	bifunctional enzyme CysN/CysC
	2.4	2.1	1.8		PA4443	sulfate adenylyltransferase subunit 2 CysD
Carbohydrate and Lipid Metabolism						
central carbohydrate metabolism	−1.5			−1.6	PA0887	acetyl-coenzyme A synthetase AcsA1
	−2.0	−1.6			PA1051	probable gluconate transmembrane transporter activity
	−1.6			−1.6	PA1984	NAD+-dependent aldehyde dehydrogenase ExaC
	−1.8			−1.6	PA4022	probable aldehyde dehydrogenase HdhA
lipid metabolism	1.7	1.7			PA2584	CDP-diacylglycerol-glycerol-3-phosphate 3-phosphatidyltransferase PgsA
	1.7				PA2969	fatty acid biosynthesis protein PlsX
Nucleotide and Amino Acid Metabolism						
aromatic amino acid metabolism	−2.0				PA2943	phospho-2-dehydro-3-deoxyheptonate aldolase
pyrimidine metabolism	−1.7				PA0443	probable transporter, permease for cytosine/purines, uracil, thiamine, allantoin
arginine and proline metabolism	−1.6				PA5170	arginine/ornithine antiporter ArcD
lysine metabolism	1.9				PA4715	probable aminotransferase YfdZ

[a]Key: CB, carbon black; MWCNT, multiwall carbon nanotubes; GNP, graphene nanoplatelets; BN, boron nitride flakes. [b]based on InterPro prediction (https://www.ebi.ac.uk/interpro/).

the culture medium, which could reduce ion bioavailability to *P. aeruginosa*, cannot be excluded, considering that MWCNTs are well-known and widely explored for their adsorption-related applications such as removal of aquatic pollutants, including heavy metal ions and organic chemicals.[46] Additionally, carbon nanotubes have been shown to alter the micronutrient content of the cell culture medium by adsorption of small-molecule solutes.[47] Another factor proposed to trigger upregulation of the genes involved in sulfur metabolism is anaerobiosis. In biofilm-grown *P. aeruginosa*, the upregulation of genes encoding sulfur assimilation (compared to planktonic cultures) was induced by prolonged anoxic conditions in the biofilms rather than sulfur starvation.[48] Here, visual and microscopic observations (Figure 1) indicated bacteria−NM heteroagglomeration in the planktonic cultures that might have caused anoxic conditions within the agglomerates and thus might have contributed to the upregulation of transcripts involved in sulfur metabolism pathways. In aerobic biofilms, low oxygen concentrations (0.01 mM) in the center of the cell clusters as thin as 80 μm have been measured experimentally by others.[49]

Carbonaceous NMs Downregulated Transcripts Involved in Nitrogen, Central Carbohydrate and Amino Acid Metabolism, and Motility/Virulence Related Functions. GNPs and MWCNTs, NMs with large hydrophobic surfaces consisting of aromatic carbon rings, commonly downregulated 16 genes and upregulated two genes (Figure 2C). Interestingly, the downregulated gene set included genes involved in assimilatory nitrate reduction (*nasA, nasS, nasT*) and a gene of an ammonium transporter *amtB*, suggesting a general down-regulatory effect of MWCNTs and GNPs on

DOI: 10.1021/acsnano.7b08977
ACS Nano 2018, 12, 2728−2740

some of the pathways in nitrogen metabolism (Table 1). It is known that, in the absence of nitrate, the sensor protein NasS inactivates antiterminator NasT, and the transcription of nitrate assimilation operons terminates at *nasAB* that encodes a nitrate transporter.[50] Here, the nitrogen source supplied in the medium was ammonium. It is therefore unclear why MWCNTs and GNPs downregulated the transcription of nitrate sensory and transport proteins in a medium lacking nitrate. Considering that many of the downregulated transcripts, including the ones involved in central carbohydrate and amino acid metabolism (Table 1), encoded cytoplasmic membrane proteins (Figures 3 and 4A), downregulation of nitrate transport genes might have

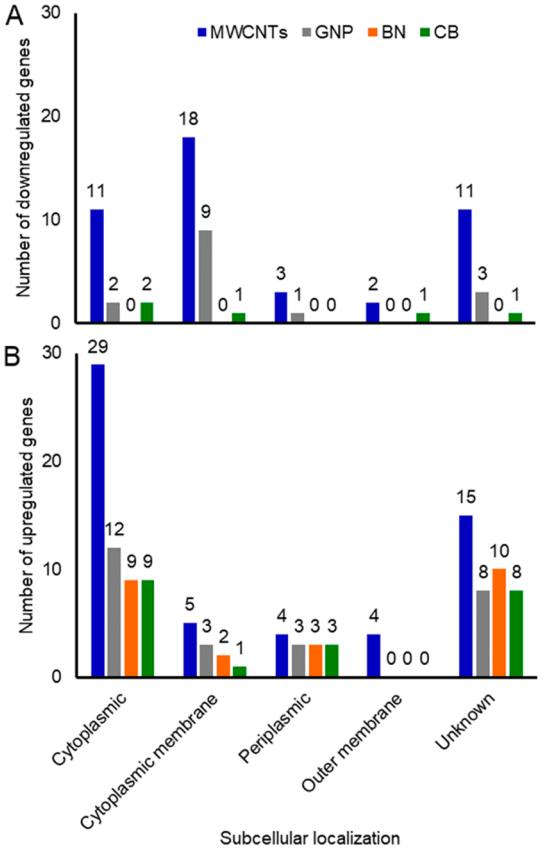

Figure 4. Subcellular localization of (A) down- and (B) upregulated genes in *P. aeruginosa* PG201 according to nanomaterial treatments. MWCNTs, multiwall carbon nanotubes; GNP, graphene nanoplatelets; BN, boron nitride flakes; CB, carbon black.

reflected a general effect of MWCNTs and GNPs on the expression of bacterial membrane proteins. Indeed, other genes regulated by MWCNTs and GNPs included genes encoding membrane transport proteins such as the probable GntP family permease (PA1051) belonging to the ion transporter superfamily, probable permeases of ABC transporters (PA4859, PA4860, PA4861), probable ATP-binding components of ABC transporters involved in monosaccharide transmembrane transport (PA0136, PA0137), and a conserved hypothetical protein (PA4858) associated with amino acid transport (Table S3). In addition, MWCNTs and GNPs both downregulated the transcription of the flagellar basal-body rod protein FlgB (PA1077) involved in flagellum-dependent swarming motility, possibly indicating reduced motility of bacteria upon agglomeration with NMs (Figure 1).

Similarly to motility, ureases are known as virulence factors in *P. aeruginosa*.[51] Among the genes regulated by GNPs and MWCNTs, a transcript encoding a urease accessory protein, UreG, was downregulated. Ureases are enzymes that catalyze the hydrolysis of urea into CO_2 and NH_3 and enable *P. aeruginosa* to colonize catheters and urinary tracts.[51] It is known that all four urease accessory proteins UreE, UreF, UreG, and UreD are necessary for the incorporation of the urease metallocenter and thus the activity of the enzyme.[52] In the urease gene cluster, *ureE*, *ureF*, and *ureG* are positioned downstream and *ureD* upstream of the urease structural genes *ureA*, *ureB*, and *ureC*. Here, the hypothetical transmembrane protein PA4894, also downregulated by GNPs and MWCNTs, and its gene located next to *ureG* in the gene cluster, was indicated to be involved in urea metabolism by *P. aeruginosa* as per the STRING Database (Figure S4). Interestingly, two downstream genes, *ureG* and PA4894, were downregulated by GNPs and MWCNTs, and the upstream gene *ureD* was upregulated by MWCNTs (Table S3). Downregulation of several urease accessory proteins was also reported in *P. aeruginosa* PA14 grown in biofilms and under anaerobic conditions.[27,48]

MWCNTs Induced a More Pronounced Transcriptomic Response As Compared to GNP, BN, and CB. MWCNTs distinctively upregulated 33 and downregulated 28 transcripts (Figure 2C). Among these, the genes belonging to the functional categories of adaptation and protection, chaperones and heat shock proteins, translation and post-translational modification, and fatty acid and phospholipid metabolism were all upregulated (Figure 3 and Table S3). Increased stress response to MWCNT exposure was implied by upregulation of several chaperones: HtpG (Hsp90), GroEL (Hsp60), 10 kDa chaperonin GroES, and DnaK (Hsp70). Chaperone ClpB, part of a stress-induced multichaperone system involved in the recovery of cells from heat-induced damage, was also upregulated, along with the ATPase subunit HslU, also known to have chaperone activity. The binding of ATP and its subsequent hydrolysis by HslU are essential for unfolding of protein substrates subsequently hydrolyzed by HslV. All of these stress response-related transcripts were upregulated in *E. coli* upon exposure to 20 mg/L MWCNTs.[9] The authors associated the upregulation of the aforementioned stress genes with membrane damage due to similar gene expression profiles induced under high pressure damage in an earlier study.[53] Relative expression of chaperone DnaK and chaperonin GroEL was increased also in a marine bacterium *Vibrio splendidus* upon exposure to 10 and 50 mg/L SWCNTs for 2 h.[54] However, Kang *et al.*[9] reported upregulation of many oxidative stress-related genes in *E. coli* upon exposure to MWCNTs, of which none were differentially regulated in the current study.

Transcripts associated with amino acid biosynthesis and metabolism, cell envelope components (wall, polysaccharides, and capsule), motility and attachment, membrane transport proteins, two-component regulatory systems, and transport of small molecules were mostly downregulated by MWCNTs (Table S3). In addition to the flagellar basal-body rod protein FlgB, which was downregulated in GNP and MWCNT treatments, MWCNTs distinctively downregulated two additional flagellar basal-body rod proteins, FlgC and FlgF, further suggesting that MWCNTs may reduce the motility and hence virulence of *P. aeruginosa*. Additionally, HsiA2, which encodes a type VI secretion-associated protein and is a component of the H2-T6SS gene cluster that plays a role in virulence and quorum

DOI: 10.1021/acsnano.7b08977
ACS Nano 2018, 12, 2728−2740

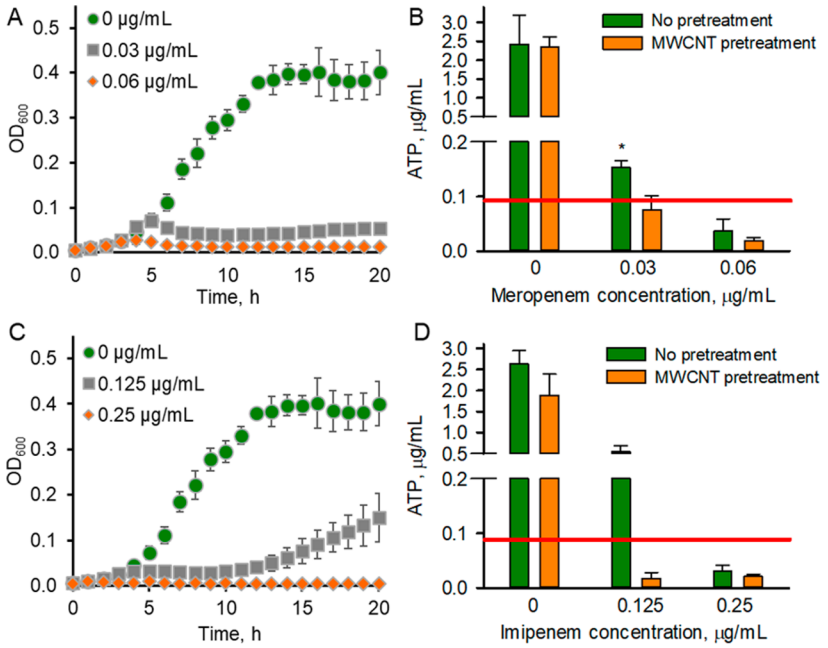

Figure 5. Susceptibility of *P. aeruginosa* PG201 to antibiotics with and without MWCNT pretreatment. Growth curves of *P. aeruginosa* in (A) meropenem and (C) imipenem exposed cultures. MICs were determined as the concentration of an antibiotic where no increase in OD_{600} was detected at 20 h compared to OD_{600} at 0 h. Inhibition of *P. aeruginosa* growth by (B) meropenem and (D) imipenem without and with 5 h MWCNT pretreatment as determined by measuring ATP concentrations in the cultures after 20-h incubation with and without antibiotics. The MIC was determined as the concentration of antibiotic where no increase in ATP concentration was detected at 20 h compared to the ATP concentration at 0 h (red lines). The MICs without MWCNT pretreatment were the same in (A, C) OD_{600}- and (B, D) ATP concentration-based assays, *i.e.*, 0.06 μg/mL of meropenem and 0.25 μg/mL of imipenem. The data are the mean values of at least three replicates and error bars indicate standard deviations. The symbol * indicates a significant difference from the ATP concentration at 0 h (red line).

sensing, was downregulated by MWCNTs. Sana *et al.* showed that the H2-T6SS machinery secretes proteins that target eukaryotic host cells and, thus, may be important in chronic *P. aeruginosa* infections in humans.[55] At the same time, the transcript abundance of Lon protease AsrA, an ATP-dependent serine protease that mediates the selective degradation of mutant and abnormal proteins as well as certain short-lived regulatory proteins, was increased. The Lon protease has also been shown to influence *P. aeruginosa* motility and biofilm formation.[56]

The functional categories that were affected distinctively by MWCNTs and not by any other treatment included a protein secretion/export apparatus, translation and post-translational modification, and two-component regulatory systems (Figure 3 and Table S3). Two-component regulatory systems are of special interest due to their role in bacterial metal and antibiotic resistance.[57]

MWCNTs Downregulated a Two-Component Regulatory System Known To Control Heavy Metal and Antibiotic Resistance. Two-component systems are signaling pathways used by bacteria to detect and respond to changing environmental conditions and stresses.[26] MWCNTs downregulated two genes that encode a two-component regulatory system, CzcR/CzcS (Figure 3 and Table S3), associated with carbapenem and heavy metal resistance and quorum sensing in *P. aeruginosa*.[58] *P. aeruginosa* is known to inhabit diverse environments and be intrinsically resistant to multiple classes of antibiotics. This characteristic could be facilitated by complex regulatory strategies including around 130 genes in the *P. aeruginosa* genome that encode two-component regulatory systems,[26] which is about twice as many as found in *E. coli*.[26] In *P. aeruginosa*, an efflux pump CzcCBA is known to contribute to the cross-resistance to heavy metals (cobalt, zinc and cadmium) and carbapenems.[58] The two-component regulatory system consisting of a transmembrane sensor kinase *czcS* and a response regulator *czcR* either represses or activates the transcription of CzcCBA, the efflux pump responsible for heavy metal resistance. It has been found that the *czcS/czcR* system coregulates the expression of *oprD* encoding a porin that is the route of entry of carbapenems.[58] Here, RNA-seq results indicated that, in addition to downregulation of *czcS/czcR* genes in *P. aeruginosa* after MWCNT exposure, *opdQ*, a gene encoding a protein belonging to the family of OprD porins, was also downregulated (Table S3). Additionally, RT-qPCR results indicated significant downregulation of *czcC*, a gene encoding a structural component of the CzcCBA efflux pump, with a relative expression ratio of 0.1 ± 0.1 (mean ± SE). However, there was no apparent downregulation of *czcS/czcR* by RT-qPCR: the relative expression ratios were 2.9 ± 2.0 and 1.9 ± 1.0, respectively, which were not significantly different from the gene expression in control *P. aeruginosa* grown without MWCNTs for 5 h. Pronounced regulation of *czcC* compared to the genes encoding regulatory proteins (*czcS/czcR*) has been reported by others: in zinc-exposed *P. aeruginosa*, *czcC* was upregulated 215-fold while the *czcS* expression level increased only 4-fold.[58] Thus, although RNA-seq and RT-qPCR results of *czcS/czcR* expression levels were not consistent, downregulation of *czcC* measured in RT-qPCR reactions was considered indicative of MWCNT interference with the two-component regulatory system of *czcS/czcR*. Considering the established role of the *czcS/czcR* two-component system in carbapenem resistance in *P. aerugino-*

DOI: 10.1021/acsnano.7b08977
ACS Nano 2018, 12, 2728−2740

sa,[58,59] we hypothesized that downregulation of *czcS/czcR* by MWCNTs would increase the susceptibility of *P. aeruginosa* to carbapenem antibiotics.

MWCNTs Increased the Susceptibility of *P. aeruginosa* PG201 to Carbapenem Antibiotics. Minimal inhibitory concentrations (MICs) of two types of carbapenems, meropenem and imipenem, in half-strength 21C medium (used in the NM exposure experiments for RNA-seq) were determined to be 0.06 and 0.25 μg/mL, respectively (Figure 5A,C). The Clinical and Laboratory Standards Institute (CLSI) reports quality control ranges for MICs of meropenem and imipenem in *P. aeruginosa* ATCCR 27853 in unsupplemented Mueller−Hinton medium as 0.25−1 and 1−4 μg/mL, respectively.[60] These values are approximately an order of magnitude higher than in the current study, which is expected, considering the use of minimal medium here. However, the relative values of MICs between the two antibiotics were comparable: *P. aeruginosa* was approximately four times more susceptible to meropenem than imipenem in this study, similar to the ratio of CLSI-reported values.

In aqueous solutions, carbonaceous NMs can readily adsorb organic compounds by hydrophobic or electrostatic interactions and affect nutrient bioavailability.[47] Also, carbonaceous NMs have been shown to modify antibiotic efficiency due to hydrophobic interactions between carbonaceous NMs and antibiotic molecules.[61] Since imipenem and meropenem lack aromatic rings in their structures and thus are not hydrophobic, their adsorption to MWCNTs was not expected (Scheme S1). This was confirmed by testing *P. aeruginosa* susceptibility to meropenem with and without cotreatment with MWCNTs: no differences in MICs were observed, suggesting that no significant adsorption of meropenem to MWCNTs occurred (Figure S5). Further, these results indicated that physical interactions of MWCNTs with bacteria that promote heteroagglomeration did not affect meropenem efficiency against *P. aeruginosa* when MWCNTs and antibiotics were added to bacterial suspensions simultaneously. To test the hypothesis that altered transcriptional regulation in the presence of MWCNTs increases antibiotic susceptibility, *P. aeruginosa* was grown with MWCNTs prior to antibiotic susceptibility testing. MWCNT-exposed culture was then used for inoculation of antibiotic treatments. Even though the amount of MWCNTs transferred with *P. aeruginosa* to the antibiotic solutions was small, MICs in the control and MWCNT pretreated *P. aeruginosa* cultures were determined by measuring ATP concentrations to avoid any interference of OD_{600} readings by MWCNTs. The MICs established for meropenem and imipenem based on OD_{600} (Figure 5A,C) and ATP measurements (Figure 5B,D) in the control cultures did not differ, confirming the suitability of ATP concentration-based MIC determination. The MICs of meropenem and imipenem in *P. aeruginosa* that had been grown with MWCNTs were lower than in unamended control cultures, suggesting that MWCNTs induced increased susceptibility to carbapenems (Figure 5B and D). In MWCNT-treated cultures, the meropenem and imipenem MICs decreased from 0.06 to 0.03 μg/mL and from 0.25 to 0.125 μg/mL, respectively. The effect on antibiotic susceptibility was MWCNT-specific, as confirmed by no change in MIC of meropenem after *P. aeruginosa* was pregrown with GNPs, CB, or BN (Figure S6). This result further indicated that the observed increased antibiotic susceptibility in MWCNT-treated bacteria likely resulted from transcriptomic changes.

Established strategies for controlling bacterial antibiotic susceptibility regulatory mechanisms include inhibiting drug efflux pumps[57] or antibiotic-degrading enzymes.[62] These approaches involve small molecule inhibitors that specifically bind to and block the active centers of the enzymes or the efflux pump channels. Recently, NMs have been studied not only for their direct antibacterial properties but as inhibitors of antibiotic degrading enzymes and chemosensitizers. Graphene oxide and carbon nanotubes were reported as inhibitors of metallo-β-lactamases, compounds that bacteria synthesize to degrade different antibiotics, including carbapenems.[63] However, the authors found that protein coating on carbonaceous NMs hindered the inhibitory properties, suggesting that graphene and CNTs would not be very effective inhibitors of metallo-β-lactamases in the environment or in human organisms that contain high concentrations of proteins and other macromolecules. Recently, two-dimensional molybdenum disulfide (MoS_2) and BN NMs at low concentrations (0.2−2 mg/L) were shown to act as chemosensitizers by inhibiting transmembrane ATP binding cassette (ABC) efflux transporter activity in human hepatoma HepG2 cells.[64] Further, MWCNTs at 50 mg/L were shown to sensitize prostate cancer cells to the chemotherapeutics docetaxel and mitomycin C when the cells were first incubated with MWCNTs for 22 h and then coincubated with MWCNTs and a chemotherapeutic for an additional 2 h.[65] In the two latter studies, NMs were internalized by cells, thereby contributing to the cytotoxicity. In the case of bacterial cells, internalization of 1D and 2D NMs is debatable, and antibacterial effects are likely manifested through contact with cell envelopes or indirect effects via changing the physicochemical properties of the culture media[66] and thereby inducing changes in transcriptional regulation. In some cases, MWCNTs exert antimicrobial properties through oxidative stress or membrane damage and thereby contribute to higher antibiotic susceptibility.[16] However, here, MWCNTs were neither growth inhibitory to *P. aeruginosa* nor induced significant membrane damage, but irrespectively sensitized bacteria to carbapenem class antibiotics. Analogously with *de novo* development of antibiotic resistance that can happen via adaptation at the gene expression level and through DNA mutations,[67] here, *P. aeruginosa* responded to MWCNT-exposure by regulating gene transcription levels that resulted in increased susceptibility to carbapenems. Due to the relatively short exposure time to MWCNTs and a modest increase (2-fold decrease in MIC) in antibiotic susceptibility, the generation of specific mutations in our study was unlikely but cannot be excluded in case of repeated long-term exposures to MWCNTs.

CONCLUSIONS

Based on the results of this study, we conclude that NMs induce transcriptional responses in *P. aeruginosa* PG201 by nonspecific interactions with the bacterial cell envelope that affect transport of small molecules into the cell and interfere with energy metabolism. Considering the subcellular localization of up- and downregulated genes, especially in case of MWCNTs, it was evident that among upregulated transcripts, cytoplasmic proteins were prevalent (Figure 4B), mostly including transcripts encoding proteins of general stress response, transcriptional regulation, transport of small molecules and central metabolism (Figure 3). On the other hand, a large fraction of genes downregulated by MWCNTs were localized in cytoplasmic and outer membrane and periplasmic

DOI: 10.1021/acsnano.7b08977
ACS Nano 2018, 12, 2728−2740

spaces (Figure 4A). These transcripts were mostly associated with membrane transport and motility (Figure 3). In addition to direct contact between NMs and bacterial cells, the changes in gene expression could be induced by indirect NM effects. NMs can affect nutrient bioavailability in the medium by adsorption.[47] Additionally, NMs may hinder nutrient availability by trapping bacteria into heteroagglomerates, resulting in reduced motility of bacteria and generation of a biofilm-like environment with lower nutrient accessibility and oxygen levels. Indicative of potentially slightly anoxic conditions were upregulation of sulfur metabolism[48] as well as no indication of upregulation of common oxidative stress related genes. MWCNTs additionally downregulated a gene encoding the OpdQ porin, reported to be transcriptionally repressed under anoxic conditions.[68]

Overall, MWCNTs induced a more pronounced transcriptomic response than GNPs, BN, and CB in the opportunistic pathogen *P. aeruginosa* PG201. MWCNTs induced specific metabolic perturbations and caused increased susceptibility to carbapenems, a class of antibiotics that are used as a last resort treatment for Gram-negative bacteria. The reason for MWCNT-specific effects could be the high aspect ratio of MWCNTs (long thin tubes) that allows for efficient wrapping around the bacterial cells[69] and heteroagglomerate formation compared to GNP and BN flakes or the small spherical CB particles at the concentration used in this study (10 mg/L). A positive correlation between the wrapping efficiency of MWCNTs around bacterial cells and nanotube toxicity has been reported previously.[13] In addition, MWCNTs were shown to have a stronger inhibitory effect on soybean root nodule development than GNPs or CB applied to soil at the same concentration.[7] Since nodules are colonized by symbiotic bacteria to enable N_2-fixation, inhibited nodule development could have been, as proposed by the authors, an indication of MWCNT effects on N_2-fixing bacteria. Our results clearly indicate that MWCNTs are more potent at inducing transcriptional changes in bacteria than other types of carbonaceous NMs such as GNPs and CB, but also 2D BN.

Considering that all studied NMs induced some level of transcriptomic response at a nongrowth-inhibitory NM concentration, our study suggests that NMs that appear relatively nontoxic when assessed by traditional toxicity end points, such as growth, could affect bacterial physiology and metabolism. Sensitive transcriptional end points shed light on subtle physiological effects of NMs that may be predictive of impacts of long-term environmental exposures but may also reveal NM effects that are potentially useful in combatting globally concerning antibiotic resistance issues.

METHODS

Nanomaterials. GNPs and MWCNTs were purchased from Cheap Tubes, Inc. (Grafton, VT), CB (Printex 30) was from Dorsett & Jackson Inc. (Los Angeles, CA), and BN flakes were from Sigma-Aldrich Inc. (Milwaukee, WI) as powders. NM stock dispersions were prepared by probe sonication in 400 mg/L of AA in nanopure water (Thermo Scientific Barnstead, Waltham, MA) as described elsewhere.[28] AA, a natural polysaccharide synthesized by certain species of algae and bacteria,[70] noncovalently coated the NMs, enabling stable aqueous dispersion of the hydrophobic NMs. NM hydrodynamic sizes and zeta potentials were measured in nanopure water and in the growth medium (Table S1). Detailed physicochemical characterization of the AA-dispersed NMs has been reported previously.[28]

Bacterial Strain and Cultivation. *P. aeruginosa* PG201 was maintained at −80 °C and cultured as described previously.[8,71,72] The bacterial inoculum was streaked from frozen stock (−80 °C, preserved in 70% Luria−Bertani [LB] broth plus 30% [v/v] glycerol) onto LB agar and cultivated in the dark (12 h, 30 °C). Several colonies were transferred from the solid media into 5 mL of minimal liquid media (half-strength 21C[73] medium which contained 0.5 g of NH_4Cl, 1.725 g of $Na_2HPO_4{\cdot}7H_20$, 1.38 g of KH_2PO_4 per L of nanopure water, 1% v/v Hutner's mineral solution,[74] and 3.4 g/L of glucose), grown aerobically to exponential phase (9 h at 30 °C, 250 rpm), transferred to a larger volume of fresh liquid medium, and grown to late exponential phase (approximately 16 h at 30 °C, 250 rpm).

Growth Assays. The cultivation of *P. aeruginosa* for determining the effects of NM exposure on growth was performed essentially as in the work of Mortimer *et al.*[8] In brief, 100 μL of half-strength 21C medium (with or without 0.1, 1, 10, or 100 mg/L NMs) was pipetted in the wells of a 96-well plate (flat-bottom polystyrene with clear bottom and sides, Corning, Inc.) and inoculated with exponential-phase *P. aeruginosa* grown as described above. For the NM treatments, the NM stock in nanopure water was diluted with 2× concentrated growth medium to obtain the final NM concentrations, pipetted into wells, and inoculated with *P. aeruginosa*. $CdCl_2$ was used as a positive control at EC_{50} concentration of 50 mg/L of Cd^{2+} (inhibited growth approximately by 50% compared to unamended culture). Each treatment, including uninoculated controls, was prepared in four replicates. The multiwell plates were incubated at 30 °C, 200 rpm in a Synergy 2 Multi-Mode microplate reader (Biotek Instruments, Winooski, VT), and optical density at 600 nm (OD_{600}) was recorded regularly over time. At 0, 2, 4, 7, and 10 h, the plates were sampled for ATP as follows (2 wells per treatment were sacrificed at each time point): ice-cold ATP extraction solution, consisting of 4% trichloroacetic acid (TCA) and 4 mM ethylenediaminetetraacetic acid (EDTA), was added into the microplate wells in 1:1 ratio with the bacterial culture, mixed by pipetting and then transferred to 1.5 mL centrifuge tubes. The tubes were vortexed and placed in ice for 10 min before transferring to −20 °C until analysis. ATP was quantified using ATP Bioluminescent Assay Kit (Sigma-Aldrich) as reported previously.[28]

Membrane Integrity Assay and Microscopy. *P. aeruginosa* was grown in microplates, as in growth assays described above, with and without 10 mg/L NMs. The membrane integrity of *P. aeruginosa* after 5-h growth was assessed using the LIVE/DEAD Bac Light Bacterial Viability Kit L7012 (Invitrogen, CA). The stocks of SYTO9, a green fluorescent nuclear stain, (3.34 mmol/L) and propidium iodide (PI, 20 mmol/L) in DMSO included in the kit were diluted in nanopure water to yield a 20× working solution (final concentrations in the assay: 4.73 μmol/L SYTO9 and 28.3 μmol/L PI). A 10 μL portion of working solution was pipetted into the wells, and the plates were incubated for 15 min in the dark at room temperature. Fluorescence was measured first at Ex/Em 485 nm/530 nm and then at 485 nm/630 nm using a Synergy 2 Multi-Mode microplate reader. For fluorescence imaging, wet mounts of stained cells were prepared and imaged immediately (Nikon E800 upright microscope with a camera and RS Image software, Roper Scientific, Trenton, NJ).

RNA Extraction, RNA-Seq Library Construction and Sequencing. *P. aeruginosa* inoculum was prepared as described above and used to inoculate 5 mL of half-strength 21C medium containing 10 mg/L NM or 20 mg/L AA in 125 mL Erlenmeyer flasks. Initial cell concentration was ~10^6 cells/mL. Bacterial cultures with or without NMs or AA were grown for 5 h at 30 °C, 250 rpm, to cell concentration ~2×10^8 cells/mL. A 10 mL portion of RNA-Protect buffer (Qiagen, MD) was added to Erlenmeyer flasks containing bacterial cultures, mixed by shaking and incubated at room temperature for 5 min. The stabilized cultures were pipetted into 15 mL centrifuge tubes (two tubes per flask) and centrifuged (10 min, 5000*g*). Supernatant was decanted, and the pellets were stored at −80 °C. The experiment was repeated on a separate day for a total of two biological replicates per each treatment. Within 24 h after freezing, RNA was extracted from thawed cell pellets using the RNeasy Mini Kit (Qiagen, MD, USA). RNA samples were DNase I-treated using the DNA-free Kit (Invitrogen). The concentration of total RNA was determined by measuring the absorbance at 280 and 260 nm using a

DOI: 10.1021/acsnano.7b08977
ACS Nano 2018, 12, 2728−2740

Cytation 3 microplate reader with a Take3Micro-Volume Plate (Biotek Instruments, VT). The concentration and quality of RNA was confirmed with a Qubit RNA BR Assay Kit using a Qubit 2.0 fluorimeter (Invitrogen). rRNA was depleted using the Ribo-Zero rRNA Removal Kit for bacteria (Epicentre, WI), and mRNA was purified using the RNA Clean & Concentrator-5 kit (Zymo Research, CA). Samples were checked for the loss of intact rRNA using TapeStation 2200 (Agilent Technologies, CA). Libraries were constructed using the TruSeq Stranded mRNA Sample Prep Kit (Illumina, CA), and 75-base pair (bp) single end sequence reads were generated using a 75 Cycle High Output NextSeq 500 platform in the Biological Nanostructures Laboratory at the California NanoSystems Institute (CNSI), University of California Santa Barbara.

RNA-Seq Data Analysis. In total, 120.2 Gb of sequencing data were obtained. Quality control assessments of the raw reads were performed using FastQC (https://www.bioinformatics.babraham.ac.uk/projects/fastqc/). Bowtie[75] was used to map the single-end reads against the *P. aeruginosa* PAO1 reference genome (GenBank accession number AE004091). The maximum number of mismatches permitted in the mapping was set to 2. Differential gene expression analysis was performed with Cuffdiff2 (version 2.2.1) from the Cufflinks package.[76] The fold change of the expression profile was measured using $\log_2$ FPKM (fragments per kilobase of transcript per million mapped reads). All genes with a $\log_2$(fold change) $\geq$ 1.4 or ≤ -1.4, and a multiple testing adjusted p-value below 0.05 were considered to be significantly modulated. Principal coordinates analysis (PCO) was performed on normalized read counts of all 12 samples.[27] Gene annotation was performed using the *Pseudomonas* Genome Database (www.pseudomonas.com)[77] and the UniProt Database (www.uniprot.org). Possible protein−protein interaction networks were checked and visualized in the STRING Database (http://string-db.org). The KEGG database (http://www.genome.jp/kegg) was used to localize the genes in *P. aeruginosa* metabolic pathways.

Determination of MICs. Minimal inhibitory concentrations (MICs) of imipenem and meropenem to *P. aeruginosa* PG201 in half-strength 21C medium were determined using the broth microdilution method.[78] *P. aeruginosa* was cultured as described above. A 50 μL portion of inoculum, prepared by diluting the pregrown culture with fresh medium to OD_{600} = 0.02, was added to 50 μL of 2× concentrated antibiotic dilution in the growth medium and pipetted into the wells of a clear polystyrene 96-well plate. Thus, the starting bacterial concentration was OD_{600} = 0.01 (~10^6 cells/mL). For controls, bacterial inoculum was mixed with unamended growth medium. Each treatment and control were prepared in at least triplicates. The multiwell plates were incubated at 30 °C, 200 rpm in a Synergy 2 Multi-Mode microplate reader, and OD_{600} was recorded regularly over time. Unamended control culture was sampled for ATP analysis at 0 h, and all the treatments were sampled for ATP after 20 h.

To determine MICs of imipenem and meropenem after MWCNT pretreatment, *P. aeruginosa* was grown with 10 mg/L MWCNTs as for the RNA-seq analysis, for 5 h. Controls were grown in identical conditions, but without the addition of MWCNTs. Pregrown *P. aeruginosa* was then used to inoculate antibiotic solutions, and MICs were determined as described above. The MIC for meropenem was also determined after *P. aeruginosa* growth with GNPs, CB or BN.

Quantitative Reverse Transcription Polymerase Chain Reaction (RT-qPCR). The relative expression of *czcC*, *czcR*, and *czcS* in MWCNT-exposed *P. aeruginosa* was measured by RT-qPCR essentially as reported previously (Supporting Information).[79,80]

Statistical Analyses. Statistical significances of means differences were determined using a two-tailed *t* test and regression analyses (Microsoft Excel, Microsoft Corporation) with a *p*-value <0.05 considered statistically significant. The EC_{50} value of Cd effect on the specific growth rate of *P. aeruginosa* was calculated using REGTOX software for Microsoft Excel (http://www.normalesup.org/~vindimian/en_download.html). The values reported throughout the text are the mean values of at least three replicate samples ± standard deviation, unless stated otherwise.

ASSOCIATED CONTENT

Supporting Information

The Supporting Information is available free of charge on the ACS Publications website at DOI: 10.1021/acsnano.7b08977.

Additional results (Figures S1−S6, Tables S1−S3) as described in the text (PDF)

AUTHOR INFORMATION

Corresponding Author

*E-mail: holden@bren.ucsb.edu.

ORCID

Monika Mortimer: 0000-0001-9008-521X

Patricia A. Holden: 0000-0002-6777-5359

Notes

The authors declare no competing financial interest.

ACKNOWLEDGMENTS

This research was funded by the National Science Foundation (NSF) and the Environmental Protection Agency (EPA) under Cooperative Agreement DBI-0830117. Any opinions, findings, and conclusions expressed in this material are those of the author(s) and do not necessarily reflect those of either the NSF or EPA. This work has not been subjected to EPA review, and no official endorsement should be inferred. The authors acknowledge the use of the Biological Nanostructures Laboratory within the California NanoSystems Institute, supported by the University of California, Santa Barbara, and the University of California, Office of the President.

REFERENCES

(1) Holden, P. A.; Klaessig, F.; Turco, R. F.; Priester, J. H.; Rico, C. M.; Avila-Arias, H.; Mortimer, M.; Pacpaco, K.; Gardea-Torresdey, J. L. Evaluation of Exposure Concentrations Used in Assessing Manufactured Nanomaterial Environmental Hazards: Are They Relevant? *Environ. Sci. Technol.* **2014**, *48*, 10541−10551.

(2) Sun, T. Y.; Bornhöft, N. A.; Hungerbühler, K.; Nowack, B. Dynamic Probabilistic Modeling of Environmental Emissions of Engineered Nanomaterials. *Environ. Sci. Technol.* **2016**, *50*, 4701−4711.

(3) Yin, J.; Li, J.; Hang, Y.; Yu, J.; Tai, G.; Li, X.; Zhang, Z.; Guo, W. Boron Nitride Nanostructures: Fabrication, Functionalization and Applications. *Small* **2016**, *12*, 2942−2968.

(4) Sun, T. Y.; Mitrano, D. M.; Bornhöft, N. A.; Scheringer, M.; Hungerbühler, K.; Nowack, B. Envisioning Nano Release Dynamics in a Changing World: Using Dynamic Probabilistic Modeling to Assess Future Environmental Emissions of Engineered Nanomaterials. *Environ. Sci. Technol.* **2017**, *51*, 2854−2863.

(5) Ge, Y.; Priester, J. H.; Mortimer, M.; Chang, C. H.; Ji, Z.; Schimel, J. P.; Holden, P. A. Long-Term Effects of Multiwalled Carbon Nanotubes and Graphene on Microbial Communities in Dry Soil. *Environ. Sci. Technol.* **2016**, *50*, 3965−3974.

(6) Holden, P. A.; Schimel, J. P.; Godwin, H. A. Five Reasons to Use Bacteria When Assessing Manufactured Nanomaterial Environmental Hazards and Fates. *Curr. Opin. Biotechnol.* **2014**, *27*, 73−78.

(7) Wang, Y.; Chang, C. H.; Ji, Z.; Bouchard, D. C.; Nisbet, R. M.; Schimel, J. P.; Gardea-Torresdey, J. L.; Holden, P. A. Agglomeration Determines Effects of Carbonaceous Nanomaterials on Soybean Nodulation, Dinitrogen Fixation Potential, and Growth in Soil. *ACS Nano* **2017**, *11*, 5753−5765.

(8) Mortimer, M.; Petersen, E. J.; Buchholz, B. A.; Orias, E.; Holden, P. A. Bioaccumulation of Multiwall Carbon Nanotubes in *Tetrahymena thermophila* by Direct Feeding or Trophic Transfer. *Environ. Sci. Technol.* **2016**, *50*, 8876−8885.

DOI: 10.1021/acsnano.7b08977
ACS Nano 2018, 12, 2728−2740

(9) Kang, S.; Mauter, M. S.; Elimelech, M. Physicochemical Determinants of Multiwalled Carbon Nanotube Bacterial Cytotoxicity. *Environ. Sci. Technol.* **2008**, *42*, 7528−7534.
(10) Perreault, F.; de Faria, A. F.; Nejati, S.; Elimelech, M. Antimicrobial Properties of Graphene Oxide Nanosheets: Why Size Matters. *ACS Nano* **2015**, *9*, 7226−7236.
(11) Arias, L. R.; Yang, L. J. Inactivation of Bacterial Pathogens by Carbon Nanotubes in Suspensions. *Langmuir* **2009**, *25*, 3003−3012.
(12) Pham, V. T. H.; Truong, V. K.; Quinn, M. D. J.; Notley, S. M.; Guo, Y.; Baulin, V. A.; Al Kobaisi, M.; Crawford, R. J.; Ivanova, E. P. Graphene Induces Formation of Pores That Kill Spherical and Rod-Shaped Bacteria. *ACS Nano* **2015**, *9*, 8458−8467.
(13) Chen, H.; Wang, B.; Gao, D.; Guan, M.; Zheng, L.; Ouyang, H.; Chai, Z.; Zhao, Y.; Feng, W. Broad-Spectrum Antibacterial Activity of Carbon Nanotubes to Human Gut Bacteria. *Small* **2013**, *9*, 2735−2746.
(14) Lu, X.; Feng, X.; Werber, J. R.; Chu, C.; Zucker, I.; Kim, J.-H.; Osuji, C. O.; Elimelech, M. Enhanced Antibacterial Activity Through the Controlled Alignment of Graphene Oxide Nanosheets. *Proc. Natl. Acad. Sci. U. S. A.* **2017**, *114*, E9793−E9801.
(15) Wang, X.; Liu, X.; Han, H. Evaluation of Antibacterial Effects of Carbon Nanomaterials Against Copper-Resistant *Ralstonia solanacearum*. *Colloids Surf., B* **2013**, *103*, 136−142.
(16) Maas, M. Carbon Nanomaterials As Antibacterial Colloids. *Materials* **2016**, *9*, 617.
(17) Vecitis, C. D.; Zodrow, K. R.; Kang, S.; Elimelech, M. Electronic-Structure-Dependent Bacterial Cytotoxicity of Single-Walled Carbon Nanotubes. *ACS Nano* **2010**, *4*, 5471−5479.
(18) Wang, X.; Mansukhani, N. D.; Guiney, L. M.; Lee, J.-H.; Li, R.; Sun, B.; Liao, Y.-P.; Chang, C. H.; Ji, Z.; Xia, T.; Hersam, M. C.; Nel, A. E. Toxicological Profiling of Highly Purified Metallic and Semiconducting Single-Walled Carbon Nanotubes in the Rodent Lung and *E. coli*. *ACS Nano* **2016**, *10*, 6008−6019.
(19) *Screening Assessment for the Challenge. Carbon Black. Chemical Abstracts Service Registry No. 1333-86-4*; Environment Canada, Health Canada, 2013; pp 20−31.
(20) Van Aken, B. Gene Expression Changes in Plants and Microorganisms Exposed to Nanomaterials. *Curr. Opin. Biotechnol.* **2015**, *33*, 206−219.
(21) Kang, S.; Herzberg, M.; Rodrigues, D. F.; Elimelech, M. Antibacterial Effects of Carbon Nanotubes: Size Does Matter. *Langmuir* **2008**, *24*, 6409−6413.
(22) Yang, Y.; Mathieu, J. M.; Chattopadhyay, S.; Miller, J. T.; Wu, T. P.; Shibata, T.; Guo, W. H.; Alvarez, P. J. J. Defense Mechanisms of *Pseudomonas aeruginosa* PAO1 against Quantum Dots and Their Released Heavy Metals. *ACS Nano* **2012**, *6*, 6091−6098.
(23) Zheng, X.; Su, Y.; Chen, Y.; Wan, R.; Li, M.; Wei, Y.; Huang, H. Carboxyl-Modified Single-Walled Carbon Nanotubes Negatively Affect Bacterial Growth and Denitrification Activity. *Sci. Rep.* **2015**, *4*, 5653.
(24) Nagy, A.; Harrison, A.; Sabbani, S.; Munson, R. S., Jr.; Dutta, P. K.; Waldman, W. J. Silver Nanoparticles Embedded in Zeolite Membranes: Release of Silver Ions and Mechanism of Antibacterial Action. *Int. J. Nanomed.* **2011**, *6*, 1833−1852.
(25) McQuillan, J. S.; Shaw, A. M. Differential Gene Regulation in the Ag Nanoparticle and Ag+-Induced Silver Stress Response in *Escherichia coli*: A Full Transcriptomic Profile. *Nanotoxicology* **2014**, *8*, 177−184.
(26) Rodrigue, A.; Quentin, Y.; Lazdunski, A.; Mejean, V.; Foglino, M. Two-Component Systems in *Pseudomonas aeruginosa*: Why So Many? *Trends Microbiol.* **2000**, *8*, 498−504.
(27) Dotsch, A.; Eckweiler, D.; Schniederjans, M.; Zimmermann, A.; Jensen, V.; Scharfe, M.; Geffers, R.; Haussler, S. The *Pseudomonas aeruginosa* Transcriptome in Planktonic Cultures and Static Biofilms Using RNA Sequencing. *PLoS One* **2012**, *7*, e31092.
(28) Wang, Y.; Mortimer, M.; Chang, C.; Holden, P. Alginic Acid-Aided Dispersion of Carbon Nanotubes, Graphene, and Boron Nitride Nanomaterials for Microbial Toxicity Testing. *Nanomaterials* **2018**, *8*, 76.
(29) Wang, H.; Adeleye, A. S.; Huang, Y.; Li, F.; Keller, A. A. Heteroaggregation of Nanoparticles with Biocolloids and Geocolloids. *Adv. Colloid Interface Sci.* **2015**, *226*, 24−36.
(30) Simon-Deckers, A.; Loo, S.; Mayne-L'Hermite, M.; Herlin-Boime, N.; Menguy, N.; Reynaud, C.; Gouget, B.; Carriere, M. Size-, Composition- and Shape-Dependent Toxicological Impact of Metal Oxide Nanoparticles and Carbon Nanotubes toward Bacteria. *Environ. Sci. Technol.* **2009**, *43*, 8423−8429.
(31) Akhavan, O.; Ghaderi, E.; Esfandiar, A. Wrapping Bacteria by Graphene Nanosheets for Isolation from Environment, Reactivation by Sonication, and Inactivation by Near-Infrared Irradiation. *J. Phys. Chem. B* **2011**, *115*, 6279−6288.
(32) Tu, Y.; Lv, M.; Xiu, P.; Huynh, T.; Zhang, M.; Castelli, M.; Liu, Z.; Huang, Q.; Fan, C.; Fang, H.; Zhou, R. Destructive Extraction of Phospholipids from *Escherichia coli* Membranes by Graphene Nanosheets. *Nat. Nanotechnol.* **2013**, *8*, 594−601.
(33) Fiume, M. M.; Bergfeld, W. F.; Belsito, D. V.; Hill, R. A.; Klaassen, C. D.; Liebler, D. C.; Marks, J. G.; Shank, R. C.; Slaga, T. J.; Snyder, P. W.; Andersen, F. A. Safety Assessment of Boron Nitride As Used in Cosmetics. *Int. J. Toxicol.* **2015**, *34*, 53S−60S.
(34) Nithya, J. S. M.; Pandurangan, A. Aqueous Dispersion of Polymer Coated Boron Nitride Nanotubes and Their Antibacterial and Cytotoxicity Studies. *RSC Adv.* **2014**, *4*, 32031−32046.
(35) Liu, S.; Wei, L.; Hao, L.; Fang, N.; Chang, M. W.; Xu, R.; Yang, Y.; Chen, Y. Sharper and Faster "Nano Darts" Kill More Bacteria: A Study of Antibacterial Activity of Individually Dispersed Pristine Single-Walled Carbon Nanotube. *ACS Nano* **2009**, *3*, 3891−3902.
(36) Yang, Y.; Xiang, Y.; Xu, M. From Red to Green: The Propidium Iodide-Permeable Membrane of *Shewanella decolorationis* S12 Is Repairable. *Sci. Rep.* **2015**, *5*, 18583.
(37) Mern, D. S.; Ha, S. W.; Khodaverdi, V.; Gliese, N.; Gorisch, H. A Complex Regulatory Network Controls Aerobic Ethanol Oxidation in *Pseudomonas aeruginosa*: Indication of Four Levels of Sensor Kinases and Response Regulators. *Microbiology* **2010**, *156*, 1505−1516.
(38) Pelletier, D. A.; Suresh, A. K.; Holton, G. A.; McKeown, C. K.; Wang, W.; Gu, B.; Mortensen, N. P.; Allison, D. P.; Joy, D. C.; Allison, M. R.; Brown, S. D.; Phelps, T. J.; Doktycz, M. J. Effects of Engineered Cerium Oxide Nanoparticles on Bacterial Growth and Viability. *Appl. Environ. Microbiol.* **2010**, *76*, 7981−7989.
(39) Chan, K. G.; Priya, K.; Chang, C. Y.; Rahman, A. Y. A.; Tee, K. K.; Yin, W. F. Transcriptome Analysis of *Pseudomonas aeruginosa* PAO1 Grown at Both Body and Elevated Temperatures. *PeerJ* **2016**, *4*, e2223.
(40) Lu, J. R.; Struewing, I.; Buse, H. Y.; Kou, J. H.; Shuman, H. A.; Faucher, S. P.; Ashbolt, N. J. *Legionella pneumophila* Transcriptional Response Following Exposure to CuO Nanoparticles. *Appl. Environ. Microbiol.* **2013**, *79*, 2713−2720.
(41) Calamita, G.; Kempf, B.; Bonhivers, M.; Bishai, W. R.; Bremer, E.; Agre, P. Regulation of the *Escherichia coli* Water Channel Gene *aqpZ*. *Proc. Natl. Acad. Sci. U. S. A.* **1998**, *95*, 3627−3631.
(42) Kahnert, A.; Vermeij, P.; Wietek, C.; James, P.; Leisinger, T.; Kertesz, M. A. The *ssu* Locus Plays a Key Role in Organosulfur Metabolism in *Pseudomonas putida* S-313. *J. Bacteriol.* **2000**, *182*, 2869−2878.
(43) Hummerjohann, J.; Kuttel, E.; Quadroni, M.; Ragaller, J.; Leisinger, T.; Kertesz, M. A. Regulation of the Sulfate Starvation Response in *Pseudomonas aeruginosa*: Role of Cysteine Biosynthetic Intermediates. *Microbiology* **1998**, *144*, 1375−1386.
(44) Tralau, T.; Vuilleumier, S.; Thibault, C.; Campbell, B. J.; Hart, C. A.; Kertesz, M. A. Transcriptomic Analysis of the Sulfate Starvation Response of *Pseudomonas aeruginosa*. *J. Bacteriol.* **2007**, *189*, 6743−6750.
(45) Scott, C.; Hilton, M. E.; Coppin, C. W.; Russell, R. J.; Oakeshott, J. G.; Sutherland, T. D. A Global Response to Sulfur Starvation in *Pseudomonas putida* and Its Relationship to the Expression of Low-Sulfur-Content Proteins. *FEMS Microbiol. Lett.* **2007**, *267*, 184−193.
(46) Das, R.; Vecitis, C. D.; Schulze, A.; Cao, B.; Ismail, A. F.; Lu, X.; Chen, J.; Ramakrishna, S. Recent Advances in Nanomaterials for

DOI: 10.1021/acsnano.7b08977
ACS Nano 2018, 12, 2728−2740

Water Protection and Monitoring. *Chem. Soc. Rev.* **2017**, *46*, 6946–7020.
(47) Guo, L.; Von Dem Bussche, A.; Buechner, M.; Yan, A.; Kane, A. B.; Hurt, R. H. Adsorption of Essential Micronutrients by Carbon Nanotubes and the Implications for Nanotoxicity Testing. *Small* **2008**, *4*, 721–727.
(48) Tata, M.; Wolfinger, M. T.; Amman, F.; Roschanski, N.; Dötsch, A.; Sonnleitner, E.; Häussler, S.; Bläsi, U. RNAseq Based Transcriptional Profiling of *Pseudomonas aeruginosa* PA14 after Short- and Long-Term Anoxic Cultivation in Synthetic Cystic Fibrosis Sputum Medium. *PLoS One* **2016**, *11*, e0147811.
(49) de Beer, D.; Stoodley, P.; Roe, F.; Lewandowski, Z. Effects of Biofilm Structures on Oxygen Distribution and Mass Transport. *Biotechnol. Bioeng.* **1994**, *43*, 1131–1138.
(50) Romeo, A.; Sonnleitner, E.; Sorger-Domenigg, T.; Nakano, M.; Eisenhaber, B.; Blasi, U. Transcriptional Regulation of Nitrate Assimilation in *Pseudomonas aeruginosa* Occurs *via* Transcriptional Antitermination within the *nirBD-PA1779-cobA* Operon. *Microbiology* **2012**, *158*, 1543–1552.
(51) Flores-Mireles, A. L.; Walker, J. N.; Caparon, M.; Hultgren, S. J. Urinary Tract Infections: Epidemiology, Mechanisms of Infection and Treatment Options. *Nat. Rev. Microbiol.* **2015**, *13*, 269–284.
(52) Lee, M. H.; Mulrooney, S. B.; Renner, M. J.; Markowicz, Y.; Hausinger, R. P. *Klebsiella aerogenes* Urease Gene Cluster: Sequence of ureD and Demonstration That Four Accessory Genes (ureD, ureE, ureF, and ureG) Are Involved in Nickel Metallocenter Biosynthesis. *J. Bacteriol.* **1992**, *174*, 4324–4330.
(53) Malone, A. S.; Chung, Y. K.; Yousef, A. E. Genes of *Escherichia coli* O157:H7 That Are Involved in High-Pressure Resistance. *Appl. Environ. Microbiol.* **2006**, *72*, 2661–2671.
(54) Berdjeb, L.; Pelletier, E.; Pellerin, J.; Gagne, J. P.; Lemarchand, K. Contrasting Responses of Marine Bacterial Strains Exposed to Carboxylated Single-Walled Carbon Nanotubes. *Aquat. Toxicol.* **2013**, *144–145*, 230–241.
(55) Sana, T. G.; Hachani, A.; Bucior, I.; Soscia, C.; Garvis, S.; Termine, E.; Engel, J.; Filloux, A.; Bleves, S. The Second Type VI Secretion System of *Pseudomonas aeruginosa* Strain PAO1 Is Regulated by Quorum Sensing and Fur and Modulates Internalization in Epithelial Cells. *J. Biol. Chem.* **2012**, *287*, 27095–27105.
(56) Breidenstein, E. B. M.; Janot, L.; Strehmel, J.; Fernandez, L.; Taylor, P. K.; Kukavica-Ibrulj, I.; Gellatly, S. L.; Levesque, R. C.; Overhage, J.; Hancock, R. E. W. The Lon Protease Is Essential for Full Virulence in *Pseudomonas aeruginosa*. *PLoS One* **2012**, *7*, e49123.
(57) Li, X.-Z.; Plésiat, P.; Nikaido, H. The Challenge of Efflux-Mediated Antibiotic Resistance in Gram-Negative Bacteria. *Clin. Microbiol. Rev.* **2015**, *28*, 337–418.
(58) Perron, K.; Caille, O.; Rossier, C.; Van Delden, C.; Dumas, J. L.; Kohler, T. CzcR-CzcS, a Two-Component System Involved in Heavy Metal and Carbapenem Resistance in *Pseudomonas aeruginosa*. *J. Biol. Chem.* **2004**, *279*, 8761–8768.
(59) Dieppois, G.; Ducret, V.; Caille, O.; Perron, K. The Transcriptional Regulator CzcR Modulates Antibiotic Resistance and Quorum Sensing in *Pseudomonas aeruginosa*. *PLoS One* **2012**, *7*, e38148.
(60) CLSI. Performance Standards for Antimicrobial Susceptibility Testing; Twenty-Second Informational Supplement. In *CLSI document M100-S22*, Clinical and Laboratory Standards Insitute: Wayne, PA, 2012.
(61) Gao, Y.; Wu, J.; Ren, X.; Tan, X.; Hayat, T.; Alsaedi, A.; Cheng, C.; Chen, C. Impact of Graphene Oxide on the Antibacterial Activity of Antibiotics against Bacteria. *Environ. Sci.: Nano* **2017**, *4*, 1016–1024.
(62) Drawz, S. M.; Bonomo, R. A. Three Decades of Beta-Lactamase Inhibitors. *Clin. Microbiol. Rev.* **2010**, *23*, 160–201.
(63) Huang, P.-J. J.; Pautler, R.; Shanmugaraj, J.; Labbé, G.; Liu, J. Inhibiting the VIM-2 Metallo-β-Lactamase by Graphene Oxide and Carbon Nanotubes. *ACS Appl. Mater. Interfaces* **2015**, *7*, 9898–9903.
(64) Liu, S.; Shen, Z.; Wu, B.; Yu, Y.; Hou, H.; Zhang, X. X.; Ren, H. Q. Cytotoxicity and Efflux Pump Inhibition Induced by Molybdenum Disulfide and Boron Nitride Nanomaterials with Sheetlike Structure. *Environ. Sci. Technol.* **2017**, *51*, 10834–10842.
(65) Erdmann, K.; Ringel, J.; Hampel, S.; Wirth, M. P.; Fuessel, S. Carbon Nanomaterials Sensitize Prostate Cancer Cells to Docetaxel and Mitomycin C *via* Induction of Apoptosis and Inhibition of Proliferation. *Beilstein J. Nanotechnol.* **2017**, *8*, 1307–1317.
(66) Kong, H. T.; Wang, L. H.; Zhu, Y.; Huang, Q.; Fan, C. H. Culture Medium-Associated Physicochemical Insights on the Cytotoxicity of Carbon Nanomaterials. *Chem. Res. Toxicol.* **2015**, *28*, 290–295.
(67) Handel, N.; Schuurmans, J. M.; Feng, Y.; Brul, S.; ter Kuile, B. H. Interaction between Mutations and Regulation of Gene Expression during Development of *De Novo* Antibiotic Resistance. *Antimicrob. Agents Chemother.* **2014**, *58*, 4371–4379.
(68) Fowler, R. C.; Hanson, N. D. The OpdQ Porin of *Pseudomonas aeruginosa* Is Regulated by Environmental Signals Associated with Cystic Fibrosis Including Nitrate-Induced Regulation Involving the NarXL Two-Component System. *MicrobiologyOpen* **2015**, *4*, 967–982.
(69) Chouhan, R. S.; Qureshi, A.; Yagci, B.; Gülgün, M. A.; Ozguz, V.; Niazi, J. H. Biotransformation of Multi-Walled Carbon Nanotubes Mediated by Nanomaterial Resistant Soil Bacteria. *Chem. Eng. J.* **2016**, *298*, 1–9.
(70) Sabra, W.; Zeng, A. P.; Deckwer, W. D. Bacterial Alginate: Physiology, Product Quality and Process Aspects. *Appl. Microbiol. Biotechnol.* **2001**, *56*, 315–325.
(71) Priester, J. H.; Stoimenov, P. K.; Mielke, R. E.; Webb, S. M.; Ehrhardt, C.; Zhang, J. P.; Stucky, G. D.; Holden, P. A. Effects of Soluble Cadmium Salts *Versus* CdSe Quantum Dots on the Growth of Planktonic *Pseudomonas aeruginosa*. *Environ. Sci. Technol.* **2009**, *43*, 2589–2594.
(72) Horst, A. M.; Neal, A. C.; Mielke, R. E.; Sislian, P. R.; Suh, W. H.; Madler, L.; Stucky, G. D.; Holden, P. A. Dispersion of TiO_2 Nanoparticle Agglomerates by *Pseudomonas aeruginosa*. *Appl. Environ. Microb.* **2010**, *76*, 7292–7298.
(73) Holden, P. A.; LaMontagne, M. G.; Bruce, A. K.; Miller, W. G.; Lindow, S. E. Assessing the Role of *Pseudomonas aeruginosa* Surface-Active Gene Expression in Hexadecane Biodegradation in Sand. *Appl. Environ. Microb.* **2002**, *68*, 2509–2518.
(74) Atlas, R. M. *Handbook of Media for Environmental Microbiology*; Taylor & Francis Group: Boca Raton, FL, 2005.
(75) Langmead, B.; Trapnell, C.; Pop, M.; Salzberg, S. L.; Ultrafast. Ultrafast and Memory-Efficient Alignment of Short DNA Sequences to the Human Genome. *Genome Biol.* **2009**, *10*, R25.
(76) Trapnell, C.; Williams, B. A.; Pertea, G.; Mortazavi, A.; Kwan, G.; van Baren, M. J.; Salzberg, S. L.; Wold, B. J.; Pachter, L. Transcript Assembly and Quantification by RNA-Seq Reveals Unannotated Transcripts and Isoform Switching during Cell Differentiation. *Nat. Biotechnol.* **2010**, *28*, 511–515.
(77) Winsor, G. L.; Griffiths, E. J.; Lo, R.; Dhillon, B. K.; Shay, J. A.; Brinkman, F. S. Enhanced Annotations and Features for Comparing Thousands of *Pseudomonas* Genomes in the *Pseudomonas* Genome Database. *Nucleic Acids Res.* **2016**, *44*, D646–D653.
(78) CLSI. *Methods for Dilution Antimicrobial Susceptibility Tests for Bacteria That Grow Aerobically; Approved Standard*; 9th ed.; Clinical and Laboratory Standards Institute: Wayne, PA, 2012.
(79) Caille, O.; Rossier, C.; Perron, K. A Copper-Activated Two-Component System Interacts with Zinc and Imipenem Resistance in *Pseudomonas aeruginosa*. *J. Bacteriol.* **2007**, *189*, 4561–4568.
(80) Devarajan, N.; Köhler, T.; Sivalingam, P.; van Delden, C.; Mulaji, C. K.; Mpiana, P. T.; Ibelings, B. W.; Poté, J. Antibiotic Resistant *Pseudomonas* spp. in the Aquatic Environment: A Prevalence Study under Tropical and Temperate Climate Conditions. *Water Res.* **2017**, *115*, 256–265.

DOI: 10.1021/acsnano.7b08977
ACS Nano 2018, 12, 2728–2740

Supporting Information for

Multiwall Carbon Nanotubes Induce More Pronounced Transcriptomic Responses in *Pseudomonas aeruginosa* PG201 than Graphene, Exfoliated Boron Nitride, or Carbon Black

Monika Mortimer[†,‡], *Naresh Devarajan*[†], *Dong Li*[†], *Patricia A. Holden*[*†,‡]

[†]Bren School of Environmental Science and Management and Earth Research Institute and [‡]University of California Center for the Environmental Implications of Nanotechnology (UC CEIN), University of California, Santa Barbara, California 93106, United States

*Corresponding Author: holden@bren.ucsb.edu, 805-893-3195 (phone), 805-893-7612 (fax).

Number of Pages: 20

Number of Figures: 6

Number of Tables: 3

METHODS

Quantitative Reverse Transcription Polymerase Chain Reaction (RT-qPCR). Total RNA was isolated from MWCNT-exposed *P. aeruginosa* as described for the RNA-seq analyses. For cDNA synthesis, 1 µg of RNA was reverse transcribed using random hexamer primers and the QuantiTect Reverse Transcription Kit (Qiagen, Germantown, MD) following the manufacturer's instructions. Reverse transcriptase was inactivated by incubation at 95 °C for 3 min. The cDNA samples were stored at -20 °C until use. The primers that were used for the PCR amplification of cDNA were selected from Caille et al.[1] A Bio-Rad CFX96 Touch Real-Time PCR Detection System (Bio-Rad Laboratories Inc., Richmond, CA) was used for the quantification of cDNA. Triplicate PCR reactions were performed using the QuantiTect SYBR Green PCR Kit (Qiagen, Germantown, MD). cDNA (500 ng/reaction) was used in a total volume of 20 µL. After a 15-min activation of the modified Taq polymerase at 95 °C, 40 cycles of 15 s at 95 °C, 20 s at 55 °C and 30 s at 72 °C were performed. Data were acquired at 72 °C. At the end of 40 cycles, a melt curve was run to test for the presence of a unique PCR reaction product. Control reactions without reverse transcriptase were analyzed using the rpsL-F/R primers[2]. The amount of signal in the controls close to the non-template control (NTC) were considered as negative for residual contamination of genomic DNA. The ribosomal *rpsL* gene (housekeeping gene in *P. aeruginosa*) was chosen to correct for the differences in the sample RNA concentrations.

Relative expression ratios were calculated according to the equation[3]:

$$ratio = \frac{(E_{target})^{\Delta CP_{target}}}{(E_{ref})^{\Delta CP_{ref}}}$$

where E_{target} is the RT-qPCR efficiency of the target gene transcript, E_{ref} is the RT-qPCR efficiency of the reference gene (*rpsL*) transcript, ΔCP_{target} is the crossing point deviation (control,

i.e., unamended *P. aeruginosa* culture, *versus* sample, i.e., *P. aeruginosa* grown with MWCNTs) of the target gene transcript, and ΔCP_{ref} is the crossing point deviation (control *versus* sample) of the reference gene transcript. RT-qPCR efficiencies were calculated according to $E = 10^{[-1/slope]}$, where slope is derived from the plot of cycle numbers of crossing points (CP) and input amounts of cDNA. An effect on gene expression was considered significant when the ratios were > 2.0 or < 0.5.[4]

RESULTS

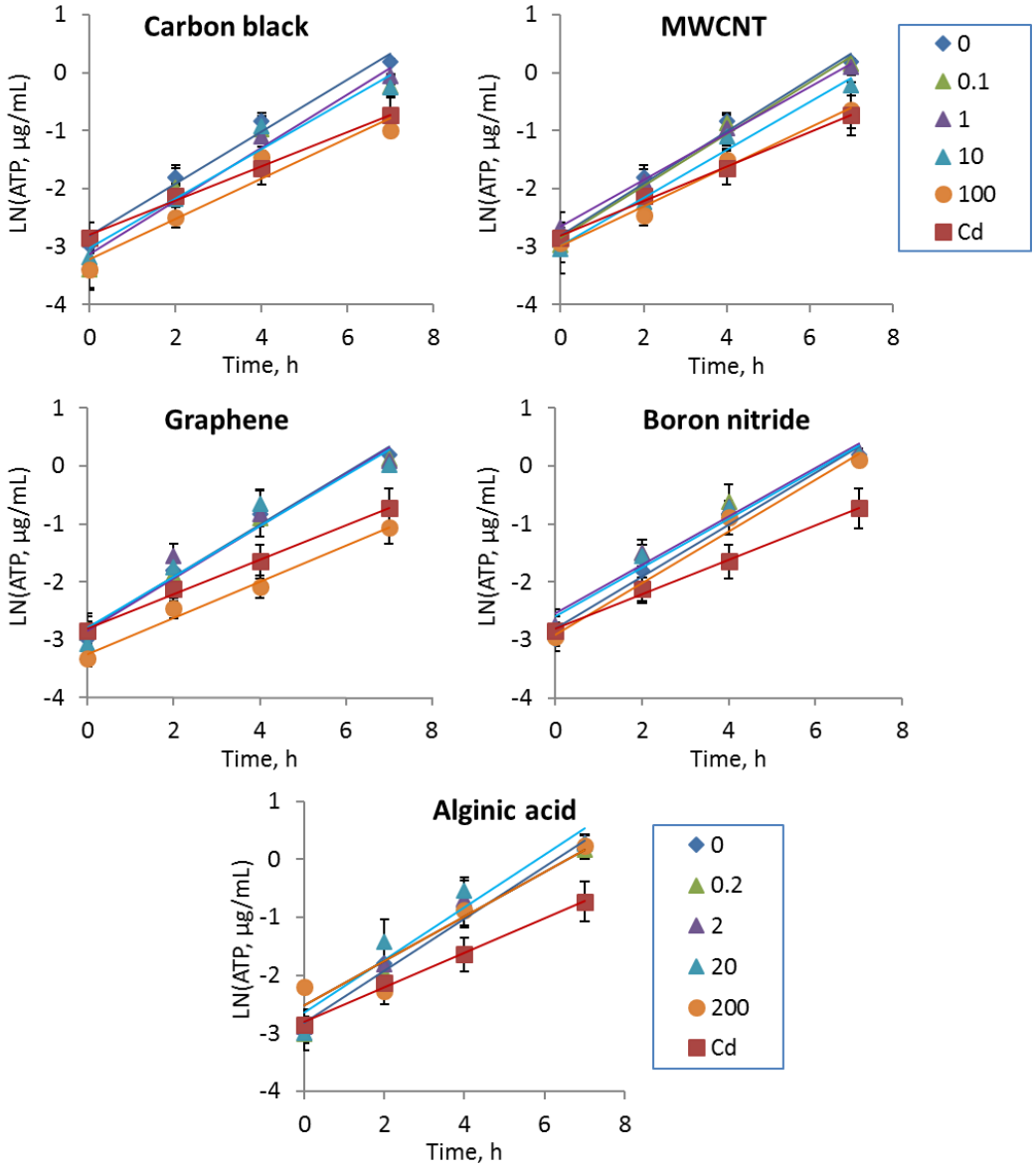

Figure S1. Natural logarithm-transformed ATP concentrations in *P. aeruginosa* cultures grown with nanomaterials at 0, 0.1, 1, 10 and 100 mg/L and with alginic acid at 0, 0.2, 2, 20 and 200 mg/L. $CdCl_2$ was used as a positive control at EC_{50} concentration of 50 mg/L of Cd^{2+} (inhibited growth approximately by 50% compared to unamended culture). Data points are the means of four replicates and error bars indicate standard deviations.

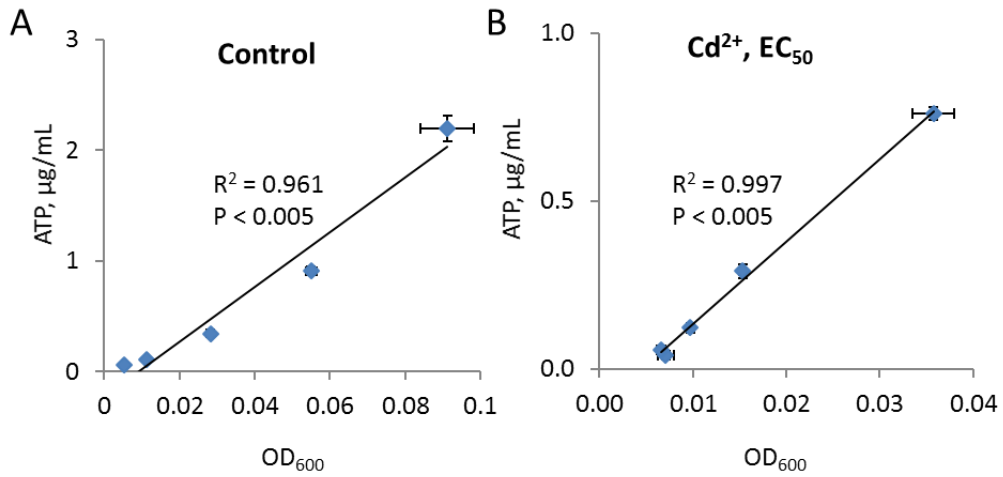

Figure S2. Plots of ATP concentrations and optical density at 600 nm (OD_{600}) in *P. aeruginosa* PG201 (A) unamended control cultures and (B) cadmium-exposed cultures over 10 h of growth in the mineral medium, showing significant positive correlations between ATP and cell concentrations in bacterial cultures over the exponential growth phase (Figure 5A and C). Data points are the average of at least four replicates and error bars indicate standard errors.

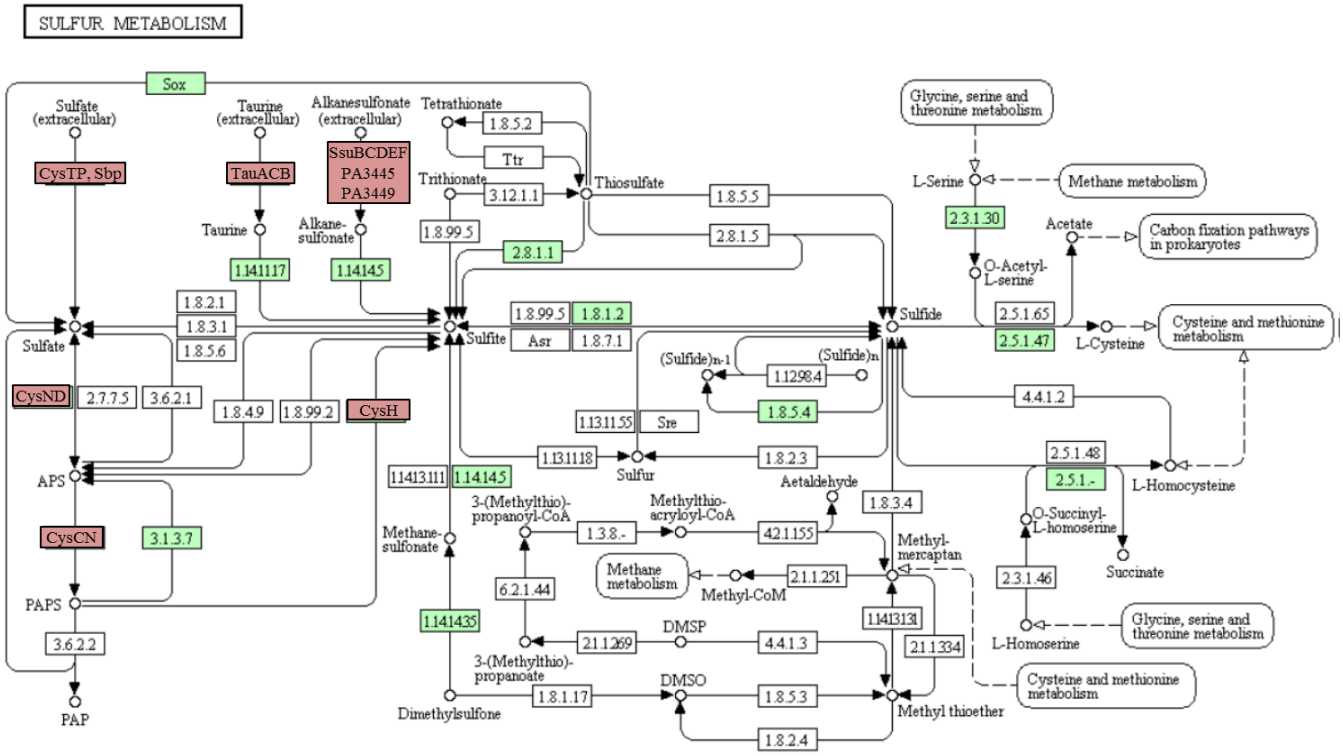

Figure S3. KEGG pathway map of sulfur metabolism in *P. aeruginosa* PAO1. The map was retrieved from http://www.genome.jp/kegg-bin/show_pathway?pae00920. The transcripts upregulated in *P. aeruginosa* PG201 upon 5-h growth in multiwall carbon nanotube (MWCNT)-amended medium in the current study are highlighted red. Some of the genes were also upregulated by graphene nanoplatelets, boron nitride flakes and carbon black (Table 1).

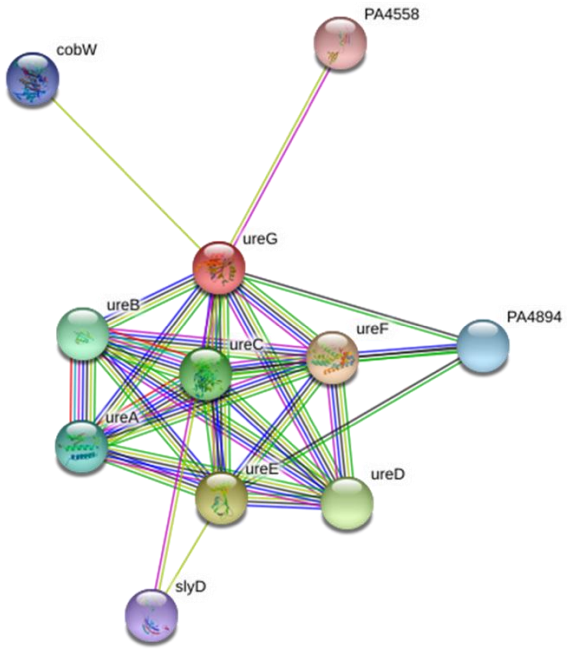

Figure S4. Network generated in the STRING database with a query of *ureG* (red node). Nodes represent proteins, edges represent protein-protein interactions. Suggested KEGG pathways: urea metabolic process. This network indicates the involvement of *ureG*, *ureD* and a hypothetical transmembrane protein PA4894, all differentially regulated in graphene and MWCNT-treated cultures, in urea metabolism by *P. aeruginosa*.

Scheme S1. Structures of meropenem (A) and imipenem (B).

A

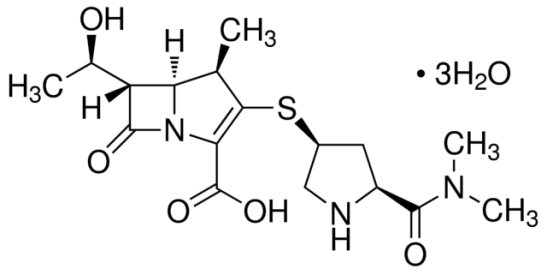

B

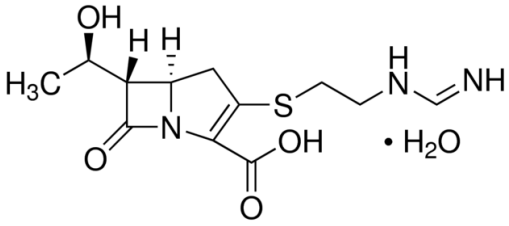

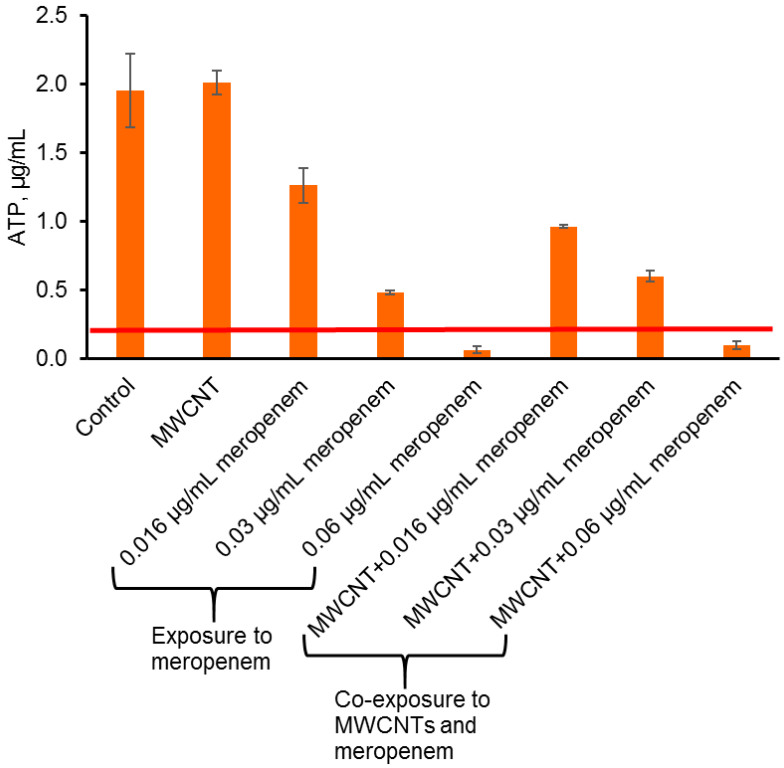

Figure S5. Susceptibility of *P. aeruginosa* PG201 to meropenem with and without 10 mg/L MWCNT co-treatment. Minimal inhibitory concentrations (MICs) were determined as the concentrations of meropenem where no increase in ATP concentration was detected at 20 h compared to ATP concentration at 0 h (red line). The bars are the average values of three replicates and error bars indicate standard deviations.

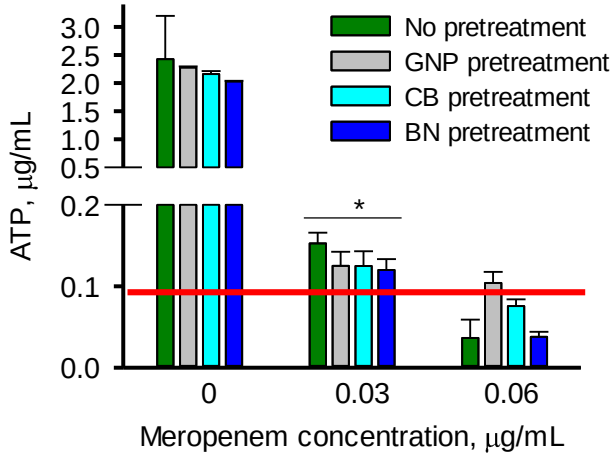

Figure S6. Inhibition of *P. aeruginosa* growth by meropenem without and with 5-h nanomaterial pretreatment as determined by measuring ATP concentrations in the cultures after 20-h incubation with and without meropenem. MIC was determined as the concentration of meropenem where no increase in ATP concentration was detected at 20 h compared to the ATP concentration at 0 h (red line). Asterisk above the black line indicates that the data bars below the line have values significantly ($p < 0.05$) greater than the ATP concentration at 0 h. GNP, graphene nanoplatelets; CB, carbon black; BN, boron nitride.

Table S1. Summary of Nanomaterial Physicochemical Characteristics.

Sample	**Catalog #**	**Size, nm**[a]	**Diameter, nm**[b]	**SSA, $m^2 g^{-1}$**[a]	**Purity, wt.%**[a]	**HDD, nm (Z-potential, mV) in nanopure water**[c]	**HDD, nm (Z-potential, mV) in growth medium**[c]
MWCNT	Sku-030106	Diameter: 30–50, length: 10000–20000	21.4 ± 6.6	60	>95	171 ± 2 (-53 ± 1)	4621 ± 606 (-36 ± 2)
GNP	GNP Grade 3	Diameter: 2000 Thickness: 8–12	1225 ± 797 (80–1600)	600–750	>97	212 ± 7 (-49 ± 2)	256 ± 4 (-33 ± 3)
BN	255475 *ALDRICH*	1000	306 ± 504	N/A	98	374 ± 18 (-65 ± 1)	460 ± 15 (-37 ± 3)
CB	PRINTEX® 30	N/A	36.6 ± 8.3	72	>99	177 ± 2 (-55 ± 0.5)	206 ± 2 (-39 ± 3)

[a]reported by the manufacturer, [b]after dispersion with alginic acid, measured from transmission electron microscopy (TEM) images following method reported in Ge et al.,[5] [c]measured using Zetasizer Nano ZS-90 (Malvern Instruments Ltd.) immediately after dispersing NMs in aqueous media, SSA – specific surface area; HDD, hydrodynamic diameter; MWCNT, multiwall carbon nanotubes; GNP, graphene nanoplatelets; BN, boron nitride flakes; CB, carbon black; N/A, not available.

Table S2. Rate Constants (k, h^{-1}; mean ± STDEV; n = 4) Calculated from the Linear Regression of Natural Log-Transformed ATP Concentrations *versus* Time (0-7 h, Figure S1).

Conc., mg/L	Treatment						
	CB	**MWCNTs**	**GNP**	**BN**	**AA**	**Control[a]**	**Cd^{2+}[b]**
0.1	0.45±0.05	0.45±0.03	0.42±0.04	0.43±0.03	0.49±0.05	0.46±0.02 (0.46±0.02)[d]	0.30±0.03[c] (0.25±0.06)[d]
1	0.46±0.02	0.40±0.03	0.45±0.01	0.42±0.05	0.49±0.04		
10	0.43±0.02	0.41±0.05	0.44±0.06	0.42±0.03	0.49±0.04		
100	0.35±0.05[c]	0.34±0.02[c]	0.31±0.05[c]	0.45±0.03	0.44±0.03		

[a]unamended culture, [b]50 mg/L Cd^{2+}, EC_{50} (inhibited growth approximately by 50% compared to control), [c]significant difference from control ($p < 0.05$), [d]specific growth rates (h^{-1}) calculated based on optical density (OD_{600}) values, not significantly different ($p > 0.05$) from the respective rate constant values calculated based on ATP concentrations. CB, carbon black; MWCNT, multiwall carbon nanotubes; GNP, graphene nanoplatelets; BN, boron nitride flakes; AA, alginic acid.

Table S3. List of Genes by Functional Classification That Were Differentially Regulated [$\log_2$(fold change) ≥1.4 or ≤-1.4] upon *P. aeruginosa* PG201 Growth with Nanomaterials for 5 h (CB, carbon black; MWCNT, multiwall carbon nanotubes; GNP, graphene nanoplatelets; BN, boron nitride flakes; AA, alginic acid).

Functional classify-cation	Gene name	Product name	Function	$\log_2$(fold change in gene expression) by treatment				
				CB	MWCNT	GNP	BN	AA
Adaptation, protection	PA3450	LsfA	Probable antioxidant protein, 1-Cys peroxiredoxin	3.0	3.5	3.7	3.9	1.7
	PA0779	Lon protease AsrA	ATP-dependent serine protease	–	2.2	–	–	–
Chaperones & heat shock proteins	PA5053	HslV	ATP-dependent protease subunit	1.7	2.4	1.7	–	–
	PA4762	GrpE	Heat shock protein, response to hyperosmotic and heat shock	1.7	2.1	1.6	–	–
	PA1596	HtpG (Hsp90)	Molecular chaperone with ATPase activity	–	2.2	–	–	–
	PA5054	HslU	ATP-dependent protease ATPase subunit	–	2.1	–	–	–
	PA4385	GroEL (Hsp60)	Molecular chaperone with ATPase activity	–	1.7	–	–	–
	PA4386	GroES	Chaperone, suppresses the ATPase activity of Mg-ATP at Hsp60	–	1.9	–	–	–
	PA4761	DnaK (Hsp70)	Chaperone	–	1.7	–	–	–
Transcrip-tional regulators	PA0191	-	Transcriptional regulator	2.2	1.8	2.5	2.5	–
	PA2312	-	Transcriptional regulator	1.5	1.6	1.9	2.0	–
	PA2334	-	Transcriptional regulator	2.3	2.2	3.0	2.6	–
	PA2359	-	Transcriptional regulator	2.1	2.6	2.8	3.2	–

Two-component regulatory systems	PA1979	EraS	Sensor kinase, ethanol oxidation	–	-1.5	–	–	–
	PA2523, PA2524	CzcR, CzcS	Carbapenem and heavy metal resistance, quorum sensing	–	-1.9	–	–	–
Amino acid biosynthesis & metabolism	PA1756	CysH	3'-phosphoadenosine-5'-phosphosulfate reductase	–	1.9	1.7	–	–
	PA2943	Phospho-2-dehydro-3-deoxy-heptonate aldolase	Stereospecific condensation of phosphoenolpyruvate and D-erythrose-4-phosphate	–	-2.0	–	–	–
Biosynthesis of cofactors, prosthetic groups and carriers	PA4893	UreG	Urea degradation II, incorporation of the urease nickel metallocenter	–	-1.5	-1.6	–	–
Carbon compound catabolism	PA1982	ExaA	Quinoprotein ethanol dehydrogenase	–	–	–	–	1.5
	PA0887	AcsA1	Conversion of acetate into acetyl-CoA	-1.6	-1.5	–	–	–
Cell wall / LPS / capsule, motility & attachment	PA1954	FapC	The main amyloid fibril monomer	1.6	–	–	–	–
	PA1077	FlgB	Flagellar basal-body rod protein	–	-1.7	-1.6	–	–
	PA1078	FlgC	Flagellar basal-body rod protein	–	-1.6	–	–	–
	PA1081	FlgF	Flagellar basal-body rod protein	–	-1.6	–	–	–
Protein secretion / export apparatus	PA1656	HsiA2	Type VI secretion-associated protein, role in virulence and quorum sensing	–	-1.4	–	–	–
	PA3105	XcpQ	Type II secretion system protein D	–	1.6	–	–	–
Translation, post-translational modification	PA4542	ClpB	Part of a stress-induced multi-chaperone system	–	1.6	–	–	–
	PA4665	PrfA	Peptide chain release factor 1, termination of translation	–	1.6	–	–	–

Fatty acid and phospho-lipid metabolism	PA2584	PgsA	CDP-diacylglycerol--glycerol-3-phosphate 3-phosphatidyltransferase	–	1.7	1.7	–	–
	PA2969	PlsX	Formation of acyl-phosphate from acyl-[acyl-carrier-protein]	–	1.7	–	–	–
Membrane proteins	PA0146	-	Conserved hypothetical protein	–	-1.6	-1.5	–	–
	PA4894	-	Hypothetical protein	–	-1.6	-2.1	–	–
	PA4779	-	EamA-like transporter family protein	–	-1.6	–	–	–
Membrane transport proteins	PA3690	Probable metal-transporting P-type ATPase	Cation-transporting ATPase activity	-1.8	-1.8	-1.7	–	–
	PA4034	AqpZ	Aquaporin Z, osmoregulation and maintenance of cell turgor in rapidly growing cells	1.5	1.6	1.7	–	–
	PA0282	CysT	ATPase-coupled sulfate transmembrane transporter activity	–	3.4	1.9	2.9	–
	PA3936,PA3937	TauC, TauB	Probable permease of ABC taurine transporter	–	2.3	–	1.5	–
	PA1051	Probable trans-porter	GntP family permease	–	-2.0	-1.6	–	–
	PA4859, PA4860, PA4861	Probable permease of ABC transporter	Transport	–	-1.5	-1.5	–	–
	PA1783	NasA	Nitrate transporter	–	-2.2	-2.3	–	–
	PA5287	AmtB	Ammonium transporter	–	-2.2	-2.0	–	–
	PA0443	Probable transporter	Permease for cytosine/purines, uracil, thiamine, allantoin	–	-1.7	–	–	–
	PA1882	Probable transporter	Small Multidrug Resistance protein	–	-1.5	–	–	–

	PA5170	ArcD	Arginine/ornithine antiporter	–	-1.6	–	–	–
	PA1651	Probable transporter		–	-1.5	–	–	–
	PA3442,PA3443	YcbE, SsuB, YcbM, SsuC	Part of the ABC transporter complex SsuABC involved in aliphatic sulfonates import	–	1.8	–	–	–
Transport of small molecules	PA0283	Sbp	ATPase-coupled sulfate transmembrane transporter activity	2.3	4.1	3.5	4.0	–
	PA2204	Probable binding protein component of ABC transporter	Ionotropic glutamate receptor activity	2.3	3.3	3.2	3.4	–
	PA3441	SsuF	Probable molybdopterin-binding protein	1.5	1.6	–	–	–
	PA3938	TauA	Probable periplasmic taurine-binding protein precursor	2.6	3.6	3.3	3.4	–
	PA4195	Probable binding protein component of ABC transporter	Transporter activity	2.2	3.2	3.1	3.1	–
	PA3939	-	Flavin adenine dinucleotide binding, oxidoreductase activity	–	1.7	–	1.8	–
	PA0136,PA0137	Probable ATP-binding component of ABC transporter	ATPase activity, ATP binding; monosaccharide transmembrane transporter activity	–	-1.9	-1.7	–	–
	PA3038	OpdQ	OprD family, outer membrane porin serving as an entry port for carbapenems	–	-1.6	–	–	–

	PA1493	CysP	Sulfate-binding protein of ABC transporter	–	1.7	–	–	–
	PA4825	MgtA	Mg(2+) transport ATPase, P-type 2	–	-2.7	–	–	–
	PA5388	CaiX	Amine and carnitine transmembrane transporter activity	–	-1.6	–	–	–
Central inter-mediary metabolism	PA4443	CysD	ATP binding, sulfate adenylyltransferase activity	–	2.4	2.1	1.8	–
	PA4864	UreD	Functional incorporation of the urease nickel metallocenter	–	1.5	–	–	–
	PA1781	Assimila-tory nitrite reductase large subunit nirB	4 iron, 4 sulfur cluster binding	–	-1.6	–	–	–
	PA1837, PA1838	Hypothe-tical protein, sulfite reductase, cysI		–	2.1	–	–	–
	PA4442	Bifunctio-nal enzyme CysN/ CysC	Adenylyl-sulfate kinase activity	–	1.8	–	–	–
Putative enzymes	PA1984	ExaC	NAD+ dependent aldehyde dehydrogenase	-1.6	-1.6	–	–	–
	PA2062	Probable pyridoxal-phosphate dependent enzyme	Catalytic activity	1.4	2.7	2.1	2.8	–
	PA4022	HdhA	Probable aldehyde dehydrogenase	-1.6	-1.8	–	–	–
	PA3444	SsuD	Alkanesulfonate monooxygenase	–	2.7	1.5	1.7	–
	PA1771	EstX	Alfa beta hydrolase	–	1.9	–	–	–
	PA4715	YfdZ	Probable aminotransferase, pyridoxal phosphate binding	–	1.9	–	–	–

	PA5546	Conserved hypothetical protein	Lipid biosynthetic process	–	-1.6	–	–	–
Unknown	PA0284	Hypothetical protein		3.2	3.2	3.9	3.8	1.8
	PA3446	Conserved hypothetical protein, ssuE	FMN reductase activity, alkanesulfonate catabolic process	3.5	3.6	4.2	4.4	2.3
	PA0201	Hypothetical protein	Hydrolase activity	2.5	2.7	3.1	3.4	–
	PA2311	Hypothetical protein		2.8	–	3.1	3.1	–
	PA2786	Hypothetical protein		2.0	2.8	3.0	2.9	–
	PA3931	Conserved hypothetical protein		2.0	–	2.2	2.7	–
	PA1333	Hypothetical protein		-1.7	-2.6	-1.9	–	–
	PA3445	Conserved hypothetical protein	Transporter activity, sulfur compound metabolic process	–	3.5	2.4	3.0	–
	PA3449	Conserved hypothetical protein	Transporter activity, sulfur compound metabolic process	–	3.0	2.0	2.6	–
	PA4824	Hypothetical protein		–	-1.7	–	1.9	–
	PA3436	Hypothetical protein		–	-2.6	-2.0	–	–
	PA4858	Conserved hypothetical protein	Amino acid transport	–	-2.3	-2.2	–	–
	PA1785	NasT	RNA binding, phosphorelay signal transduction system, regulation of nitrate assimilation	–	-1.9	-2.0	–	–
	PA1786	NasS	Sensor activity	–	-1.7	-1.8	–	–
	PA0377	Hypothetical protein		–	1.6	–	–	–
	PA1730	Conserved hypothetical protein		–	-1.6	–	–	–
	PA2043	Hypothetical protein		–	1.7	–	–	–
	PA2381	Hypothetical protein		–	-2.4	–	–	–
	PA2433	Hypothetical protein		–	-1.6	–	–	–

	PA2604	Conserved hypothetical protein	Negative regulation of apoptotic process	–	-1.6	–	–	–
	PA3202	Conserved hypothetical protein		–	1.5	–	–	–
	PA3263	Recombination-associated protein RdgC	May be involved in recombination	–	1.5	–	–	–
	PA3981,PA3982,PA3983	Conserved hypothetical protein, endoribonuclease YbeY	ATP binding; single strand-specific metallo-endoribonuclease	–	1.8	–	–	–
	PA3990	Conserved hypothetical protein		–	-1.7	–	–	–
	PA4063	Hypothetical protein		–	2.1	–	–	–
	PA4090	Hypothetical protein		–	1.5	–	–	–
	PA4354	Conserved hypothetical protein	Regulation of single-species biofilm formation on inanimate substrate; regulation of transcription	–	-1.7	–	–	–
	PA4635	Conserved hypothetical protein		–	-1.6	–	–	–
	PA5055	Hypothetical protein		–	1.5	–	–	–
	PA0389	Hypothetical protein	Methylation	–	1.5	–	–	–
	PA0948	Hypothetical protein		–	1.6	–	–	–
	PA1331	Conserved hypothetical protein	Flavin adenine dinucleotide binding; oxidoreductase activity	–	1.8	–	–	–
	PA1913	Hypothetical protein		–	2.0	–	–	–
	PA2021	Hypothetical protein		–	-1.5	–	–	–
	PA2289	Conserved hypothetical protein	Transport	–	1.6	–	–	–

	PA4575	Hypothetical protein	–	-1.8	–	–	–
	PA4824	Hypothetical protein	–	-1.7	–	–	–
	PA4826	Hypothetical protein	–	-2.6	–	–	–

References

1. Caille, O.; Rossier, C.; Perron, K., A Copper-Activated Two-Component System Interacts with Zinc and Imipenem Resistance in *Pseudomonas aeruginosa*. *J. Bacteriol.* **2007,** *189*, 4561-4568.
2. Devarajan, N.; Köhler, T.; Sivalingam, P.; van Delden, C.; Mulaji, C. K.; Mpiana, P. T.; Ibelings, B. W.; Poté, J., Antibiotic Resistant *Pseudomonas* spp. in the Aquatic Environment: A Prevalence Study under Tropical and Temperate Climate Conditions. *Water Res.* **2017,** *115*, 256-265.
3. Pfaffl, M. W., A New Mathematical Model for Relative Quantification in Real-Time RT-PCR. *Nucleic Acids Res.* **2001,** *29*, e45.
4. Perron, K.; Caille, O.; Rossier, C.; Van Delden, C.; Dumas, J. L.; Kohler, T., CzcR-CzcS, a Two-Component System Involved in Heavy Metal and Carbapenem Resistance in *Pseudomonas aeruginosa*. *J. Biol. Chem.* **2004,** *279*, 8761-8768.
5. Ge, Y.; Priester, J. H.; Mortimer, M.; Chang, C. H.; Ji, Z.; Schimel, J. P.; Holden, P. A., Long-Term Effects of Multiwalled Carbon Nanotubes and Graphene on Microbial Communities in Dry Soil. *Environ. Sci. Technol.* **2016,** *50*, 3965-3974.